Looking for mergers in gravitational wave data: results, lessons, and future outlook

Tejaswi Venumadhav

University of California
Santa Barbara

$d(t)$

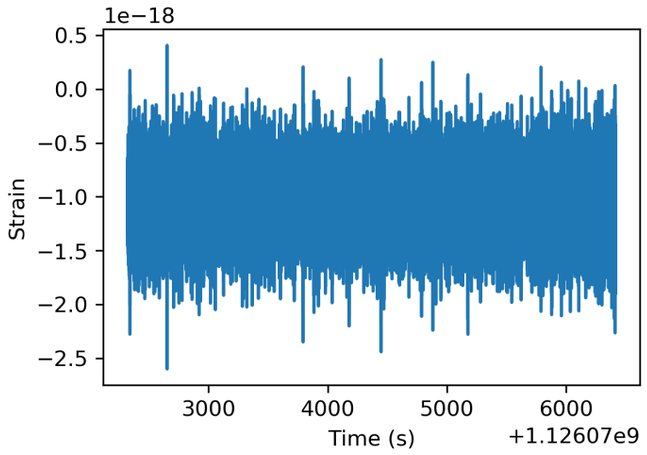

Data

$h(t)$

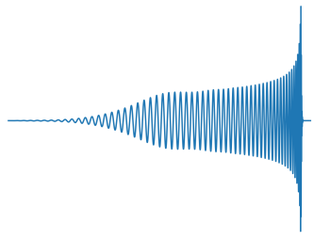

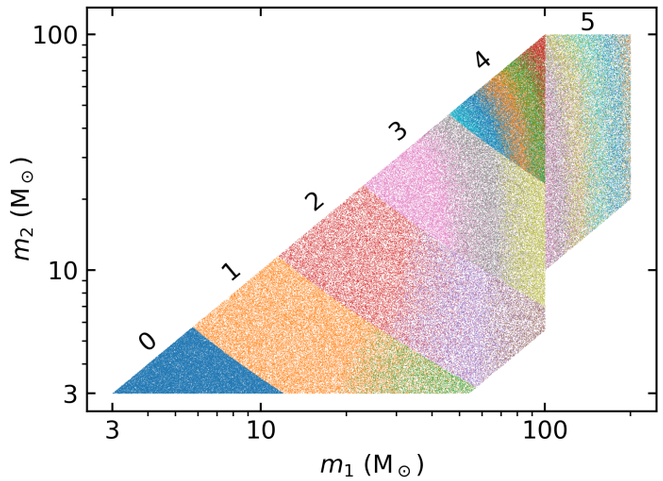

Signal model

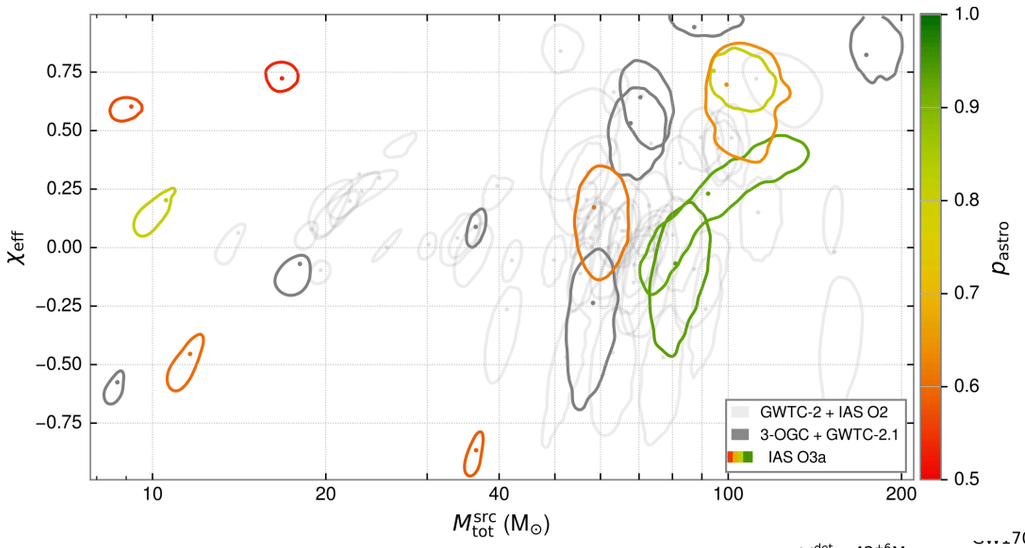

Population inference

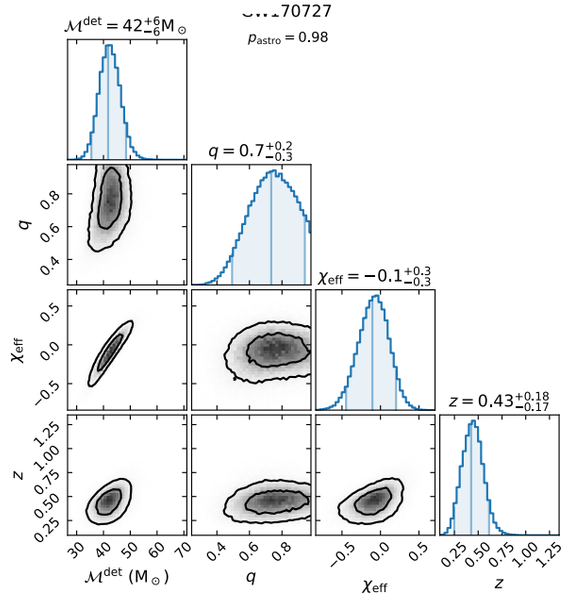

Parameter estimation

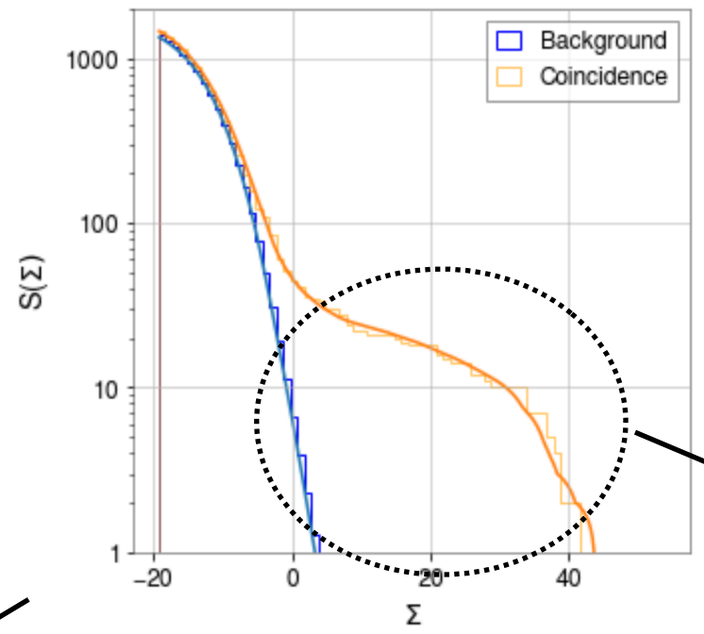

Summary statistic + Triggers

Candidates

Tejaswi Venumadhav

GW from binaries: source properties

Amplitude

$$h_{ij} \sim \frac{1}{R}\ddot{q}_{ij} \sim 10^{-21}\left(\frac{\omega_{GW}}{100\,\mathrm{Hz}}\right)^{2/3}\left(\frac{M_c}{25\,M_\odot}\right)^{5/3}\left(\frac{400\,\mathrm{MPc}}{R}\right)$$

$$M_c = \frac{(m_1 m_2)^{3/5}}{(m_1+m_2)^{1/5}}$$ "chirp" mass

Frequency

$$\omega_{\mathrm{GW}}(t) \sim M_c^{-5/8}\left(t_0 - t\right)^{-3/8}$$ "Chirping" behavior

$$t_0 - t_{\min} \sim \frac{1}{M_c^{5/3}\omega_{\mathrm{GW,min}}^{8/3}} \approx 0.5\,s\left(\frac{25\,M_\odot}{M_c}\right)^{5/3}\left(\frac{20\,\mathrm{Hz}}{\omega_{\min}}\right)^{8/3}$$

$$\omega_{\max} \sim 100\,\mathrm{Hz}\left(\frac{50\,M_\odot}{M}\right)$$ Cutoff at ISCO

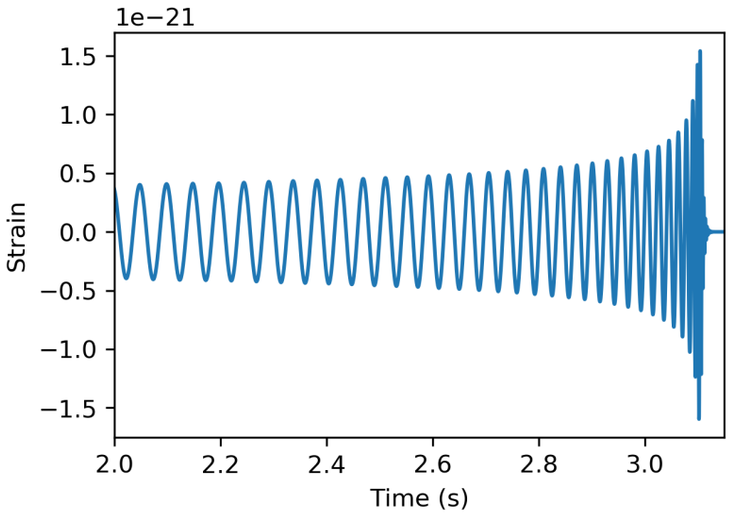

Orbital phase and waveforms

$$\phi(\omega_{\mathrm{GW}}) \sim \int \omega_{\mathrm{GW}}(t)\,dt \sim \left(\frac{1}{M_c\,\omega_{\mathrm{GW}}}\right)^{5/3}$$

$$h(\omega_0) = \int dt\, h(t)\, e^{-i\omega_0 t} \sim \omega_0^{-7/6} e^{i\phi(\omega_0)}$$

SPA

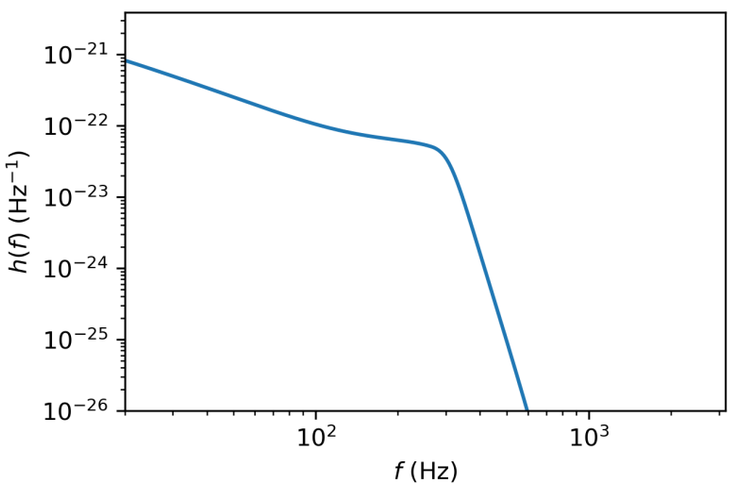

Gaussian noise model: matched filtering

$h(t)$

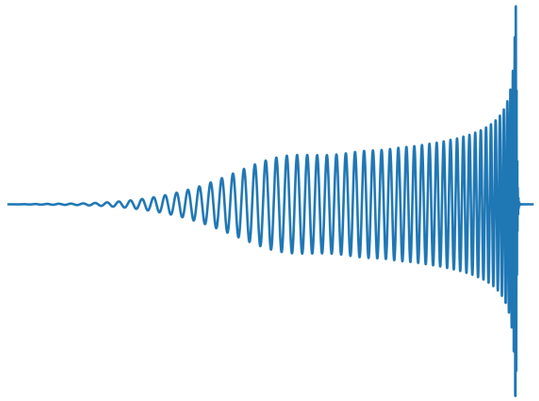

$d(t)$

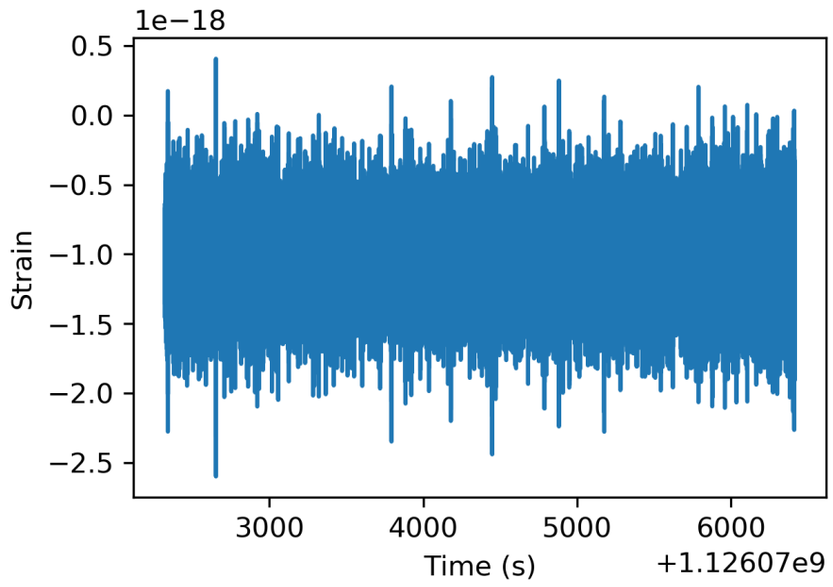

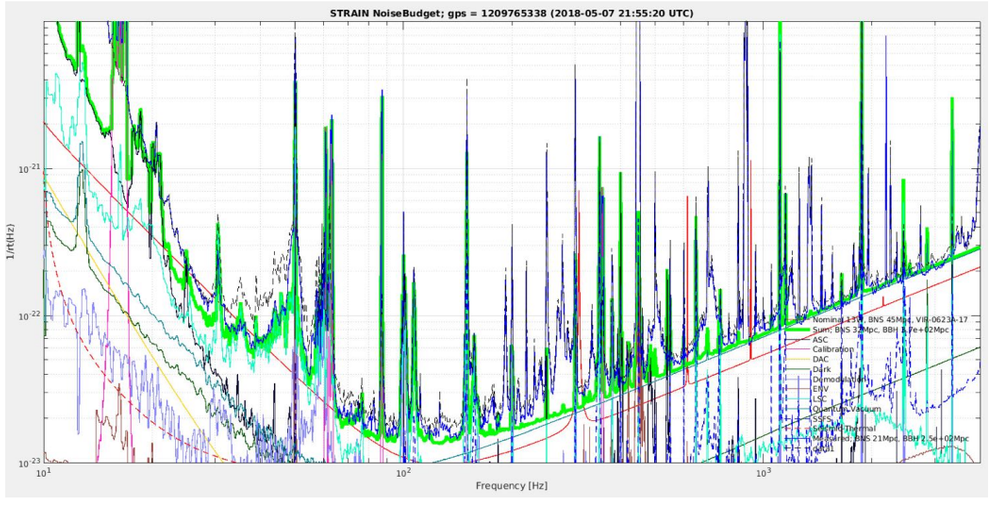

Credit: Giovanni Losurdo

Simplest case is stationary Gaussian random noise

$$\langle d(t+\tau)d(t)\rangle = C(\tau)$$

FT of $C(\tau)$ is the PSD $S(f) \sim \sigma^2(f) \equiv \langle |d(f)|^2 \rangle$

We have to estimate $S(f)$ ourselves!

Define (`whitening filter') $1/\sigma(f)$ such that filtered data

$$w(f) = \frac{d(f)}{\sigma(f)}$$

has white noise statistics

The matched-filtering score is the convolution of the whitened data with the whitened template

$$\rho = \frac{\frac{\sum_f d(f)h^\star(f)}{\sigma^2(f)}}{\left[\frac{\sum_f |h(f)|^2}{\sigma^2(f)}\right]^{1/2}}$$

Behaves like SNR

Collect coincident and background events

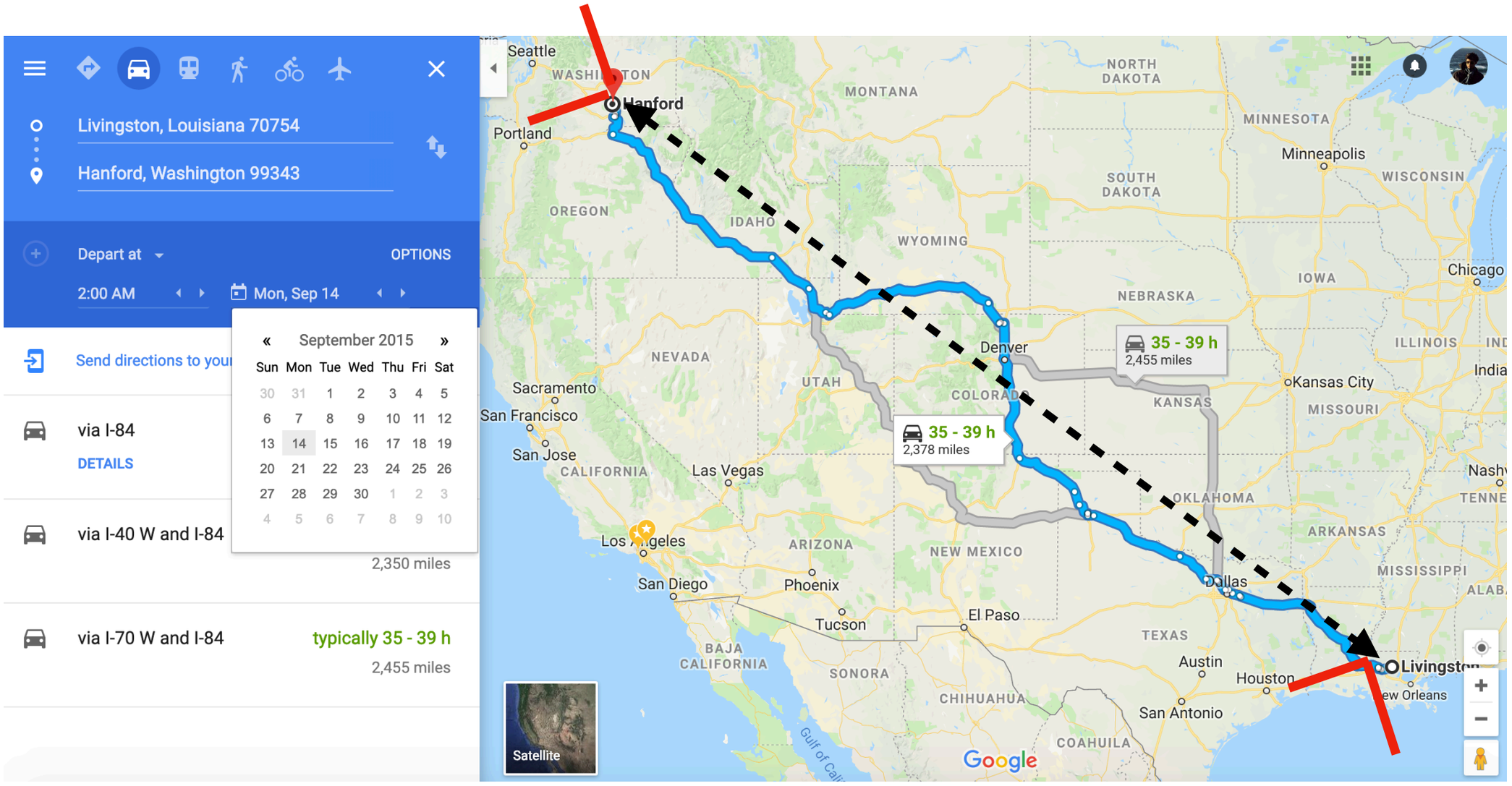

Shift data stream by t > 10 ms
to estimate background

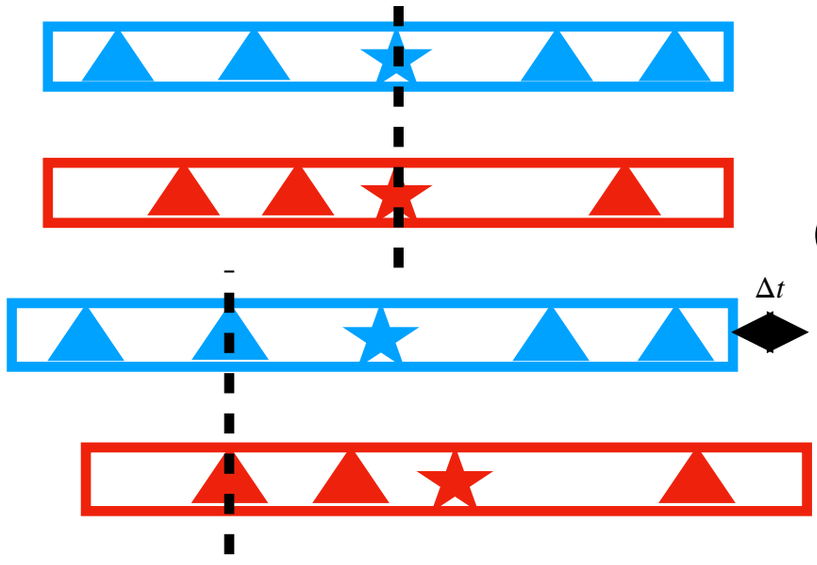

Credit: Ian Harry

Tejaswi Venumadhav

Detection criteria (O2)

1. False alarm rate (FAR) < 1 in 30 days

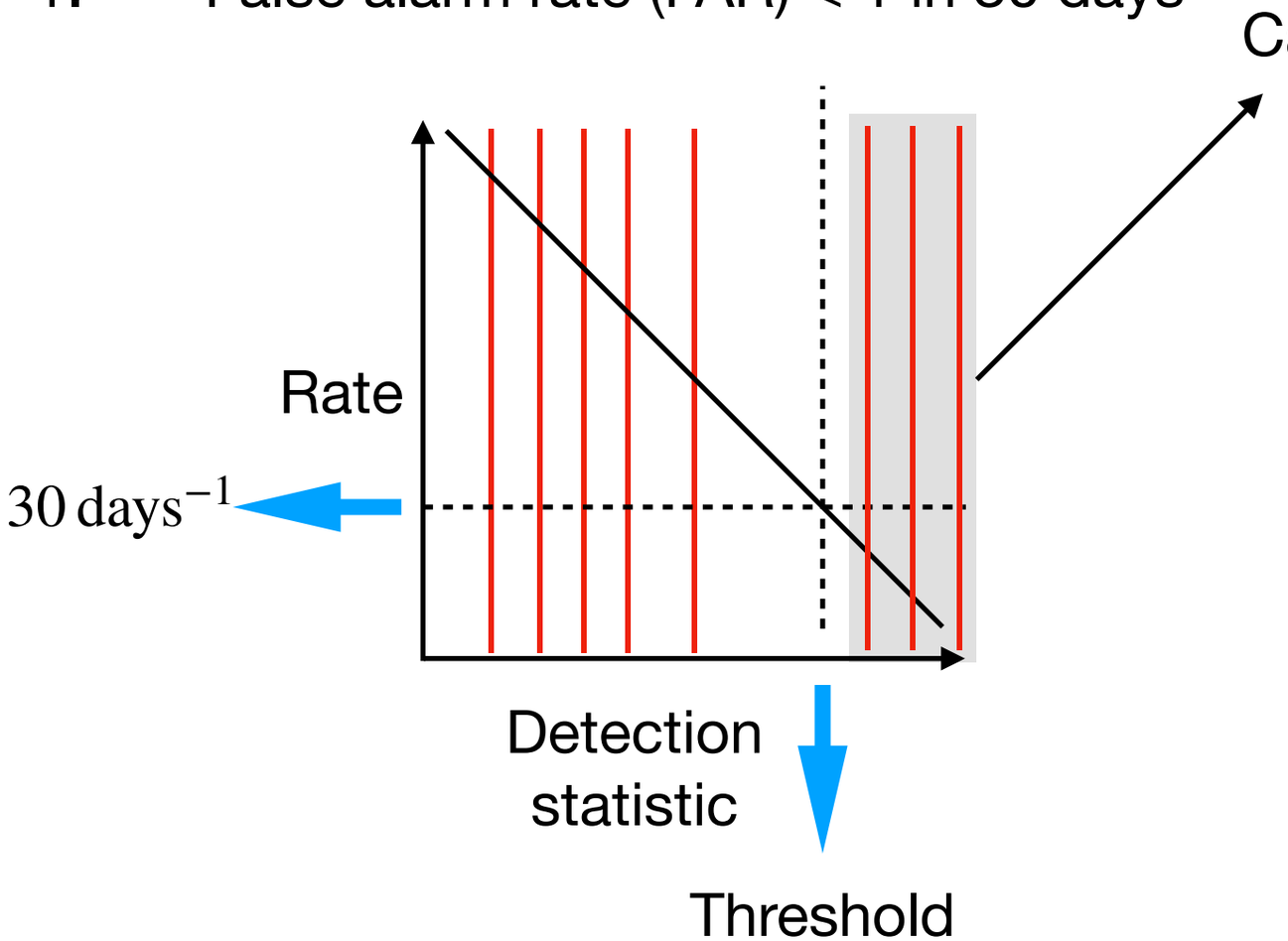

e.g.: SNR^2 should be distributed according to a chi-squared distribution

2. $$p_{\mathrm{astro}} = \frac{R\left(\mathrm{candidate} \mid \mathcal{S}\right)}{R\left(\mathrm{candidate} \mid \mathcal{N}\right) + R\left(\mathrm{candidate} \mid \mathcal{S}\right)} > 0.5$$

Abbott et. al. (2018)
arxiv:1811.12907

Template bank

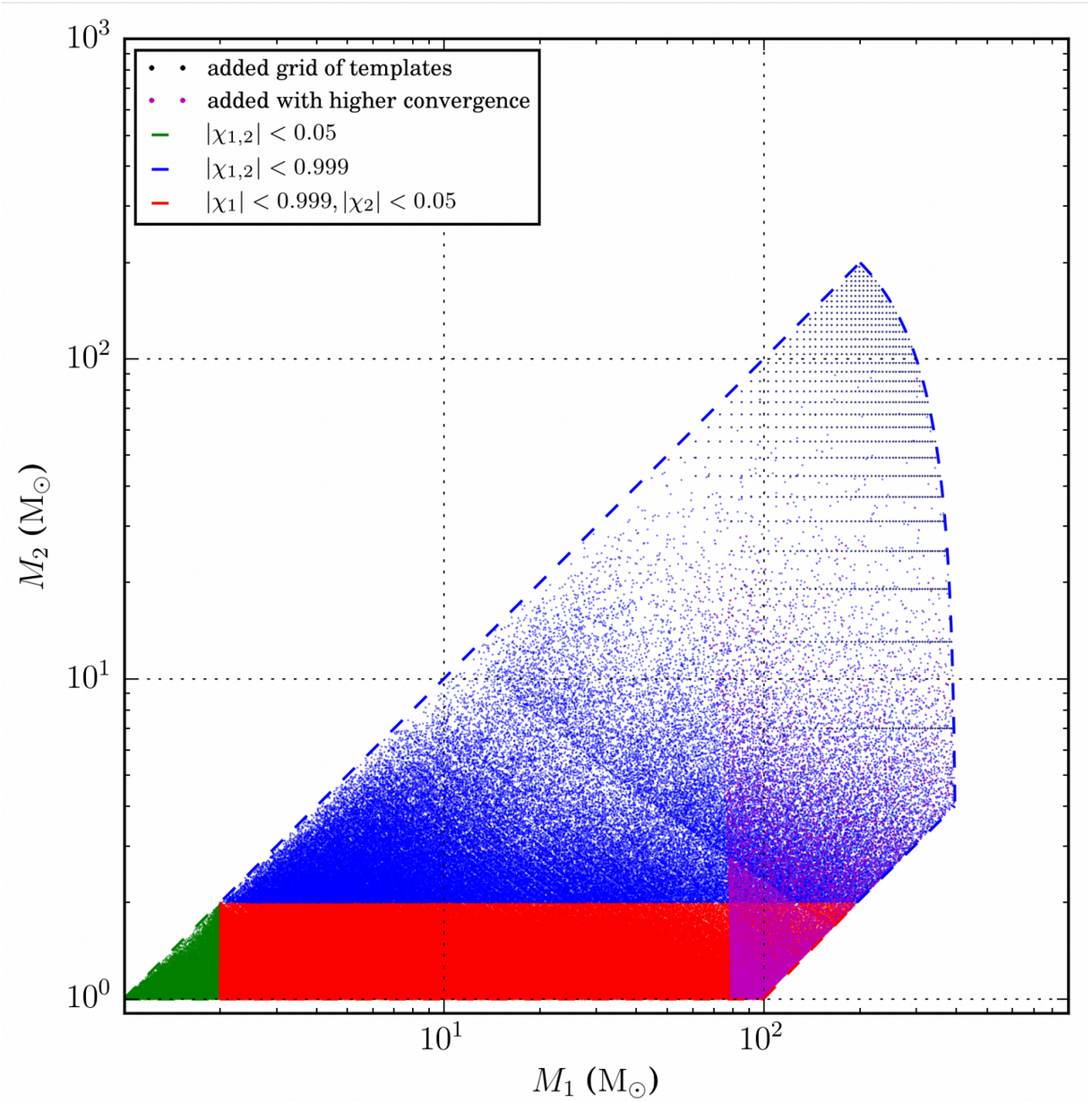

Sachdev et. al., (2019)
arxiv: 1901.08580

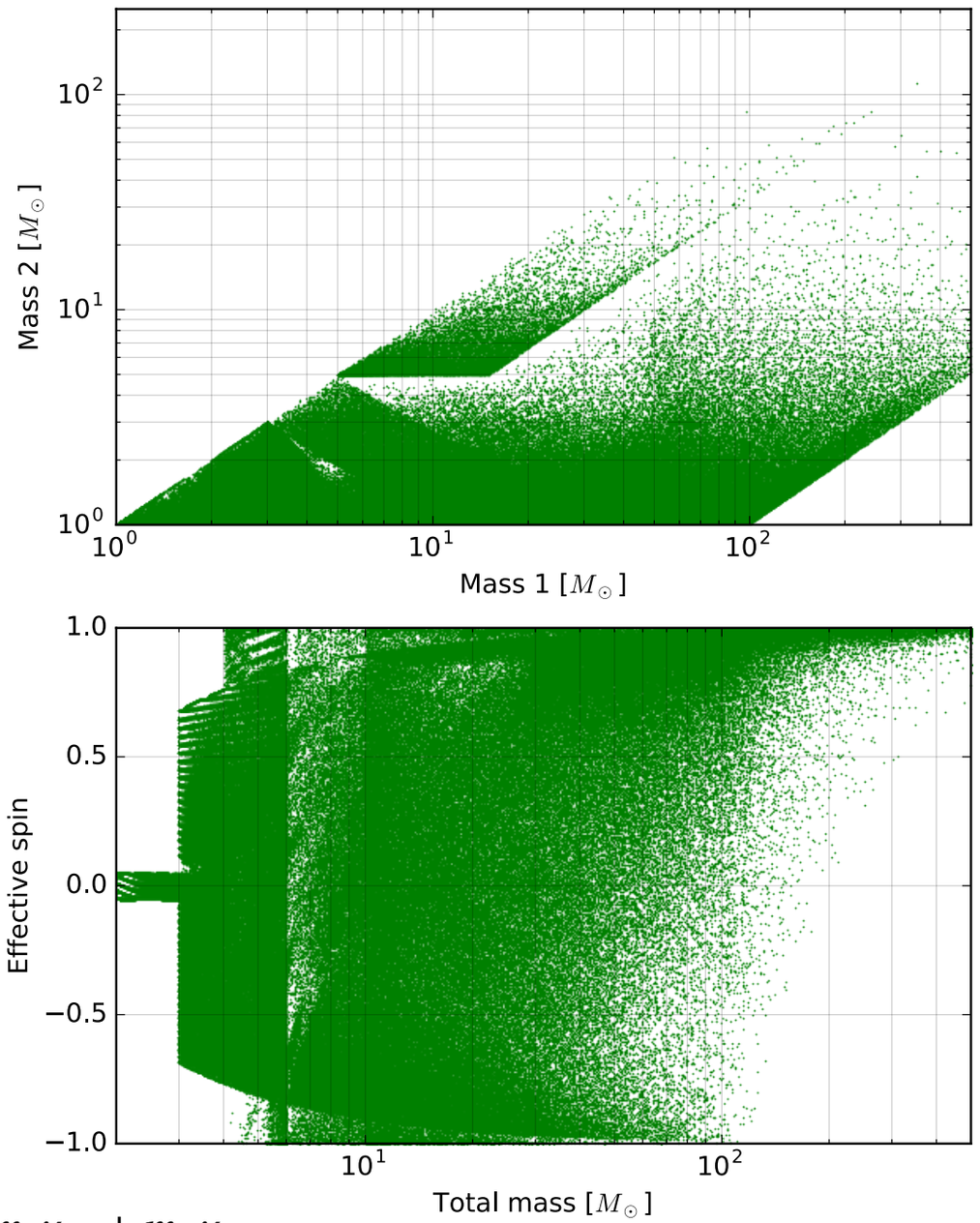

$$\chi_{\text{eff}} = \frac{m_1\chi_{1,z} + m_2\chi_{2,z}}{m_1 + m_2}$$

Canton and Harry (2017)

Template bank

Canton and Harry (2017)

$$z(h) = \sum_f \frac{d(f)h^\star(f)}{\sigma^2(f)}$$

$$h(f) \sim f^{-7/6} e^{i\phi(f)}$$

$$\phi \sim \frac{1}{\left(M_c f_{\min}\right)^{5/3}}$$

$$\frac{d\mathrm{N}}{d\ln M_c} \sim \left(M_c f_{\min}\right)^{-5/3}$$

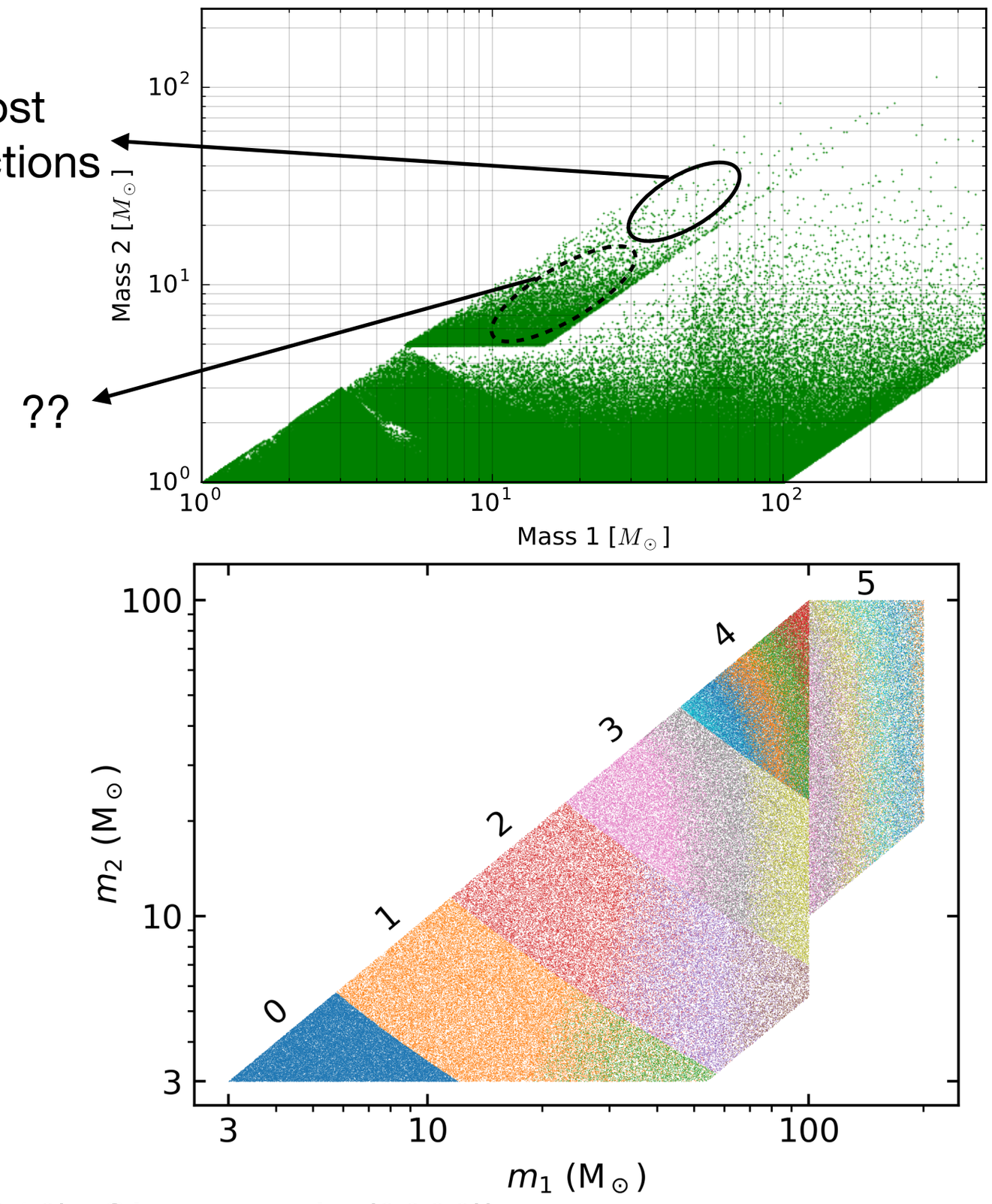

Solution:

Template prior
(Dent, T., and Veitch, J., (2014)

Multiple banks (Roulet et. al., (2019), Olsen et. al., (2022))

Systematic: non-stationary noise

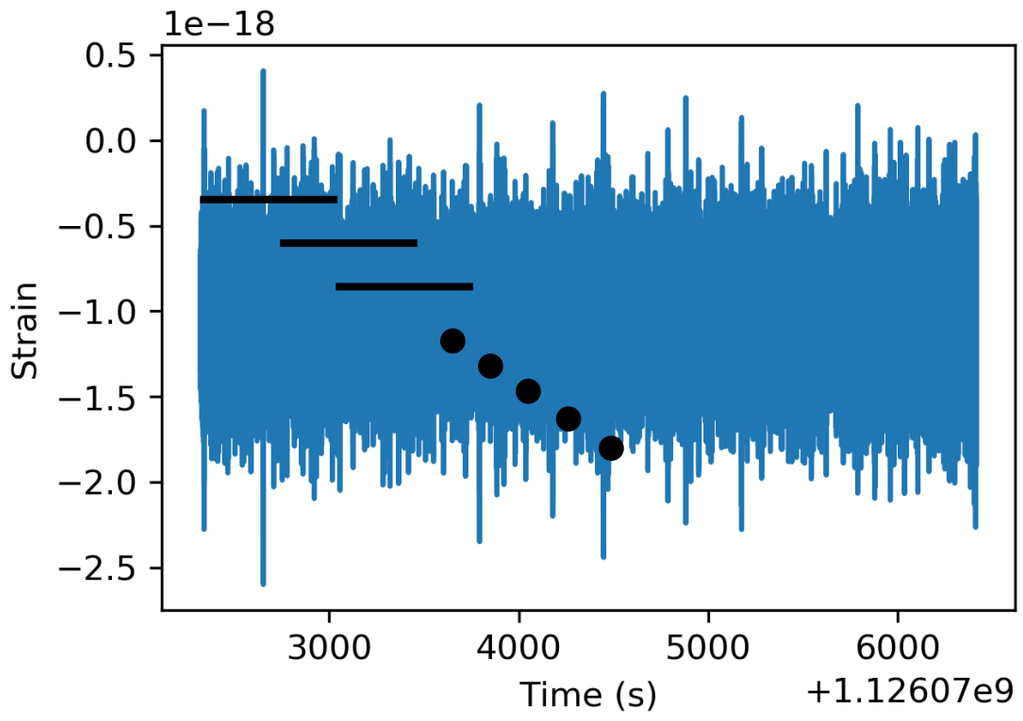

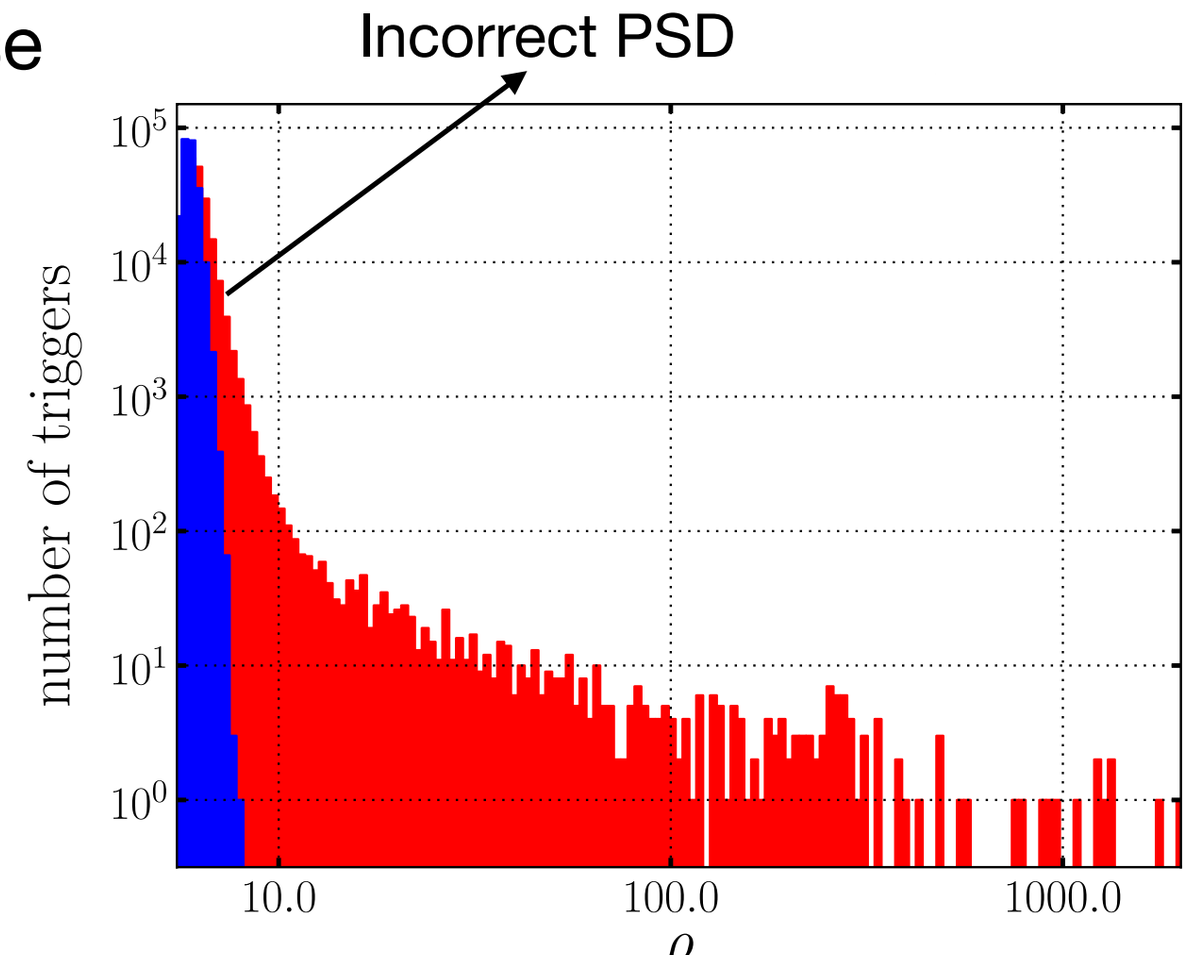

$$\frac{Z}{\sigma_Z} = \frac{\sum_f \frac{h^*(f)d(f)}{\sigma^2(f)}}{\sqrt{\sum_f \frac{|h(f)|^2}{\sigma^2(f)}}}$$

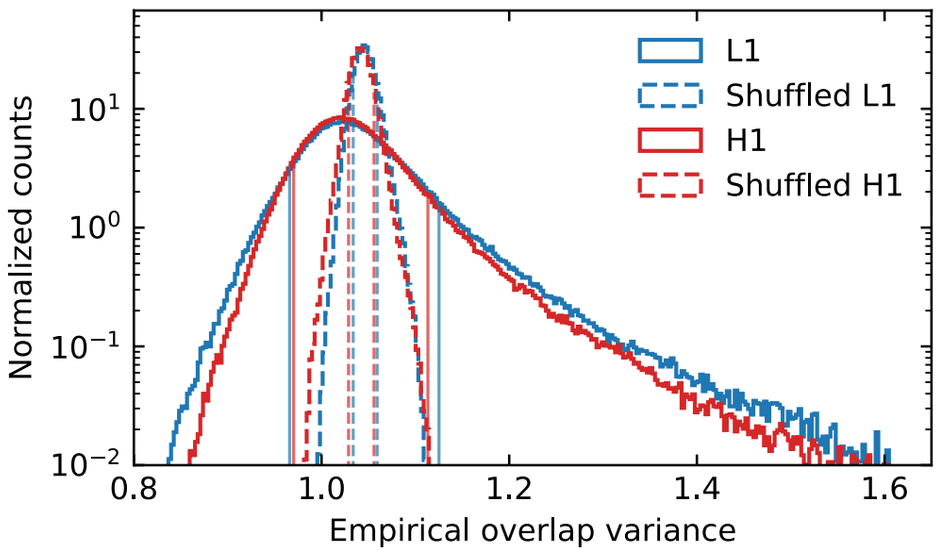

$$\langle d(t+\tau)d(t)\rangle = C(\tau) \longrightarrow \langle d(t+\tau/2)d(t-\tau/2)\rangle = C(\tau,t) \approx C(\tau)f(t)$$

Zackay et. al., (2021) **Tejaswi Venumadhav**

Glitches

$$z(h) = \sum_f \frac{d(f)h^\star(f)}{\sigma^2(f)}$$

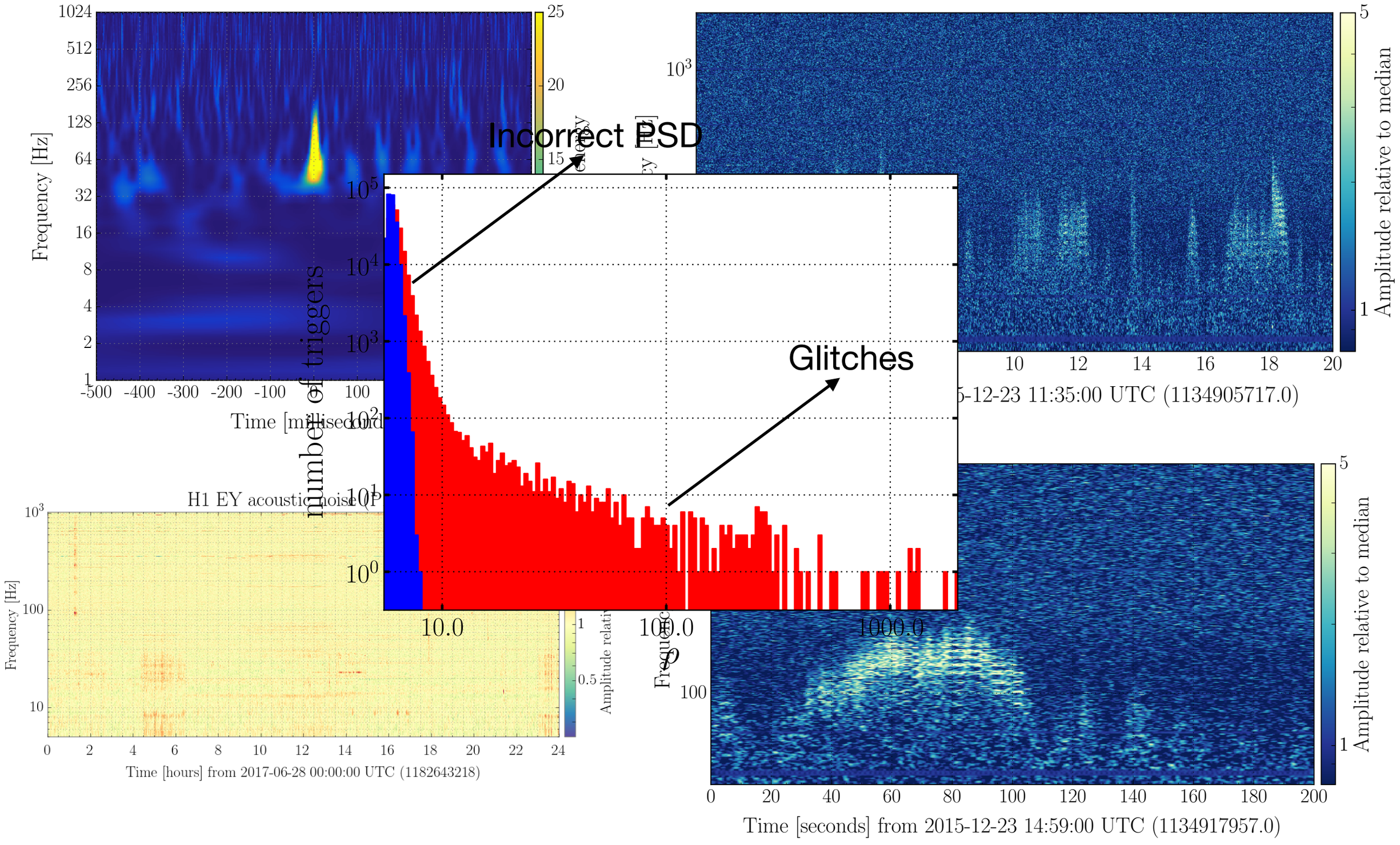

Image: Beverly Berger

Abbott et. al. (2017)

Glitches

$$z(h) = \sum_f \frac{d(f)h^\star(f)}{\sigma^2(f)} \longrightarrow p(z)$$

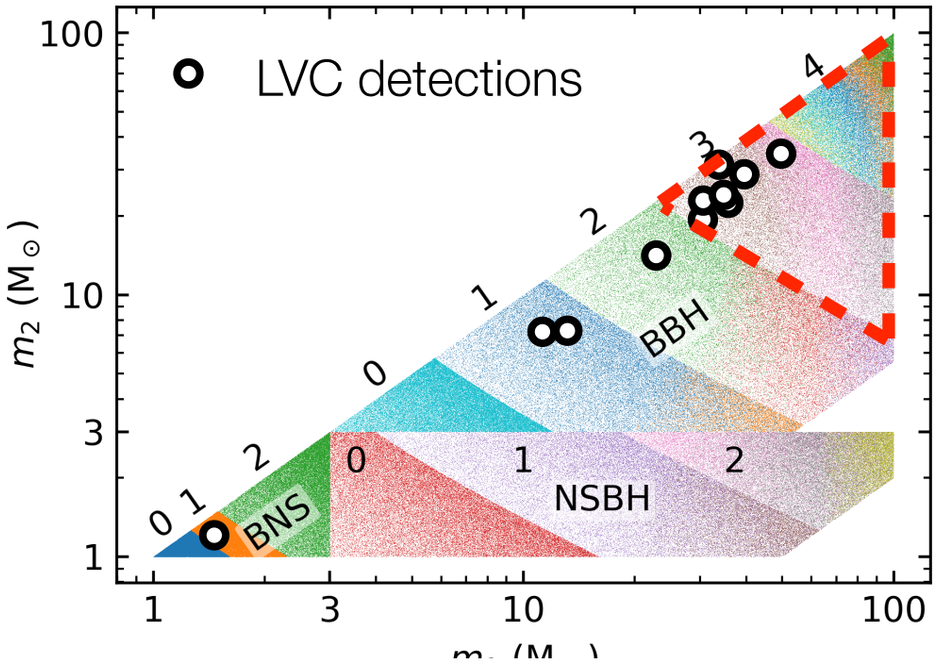

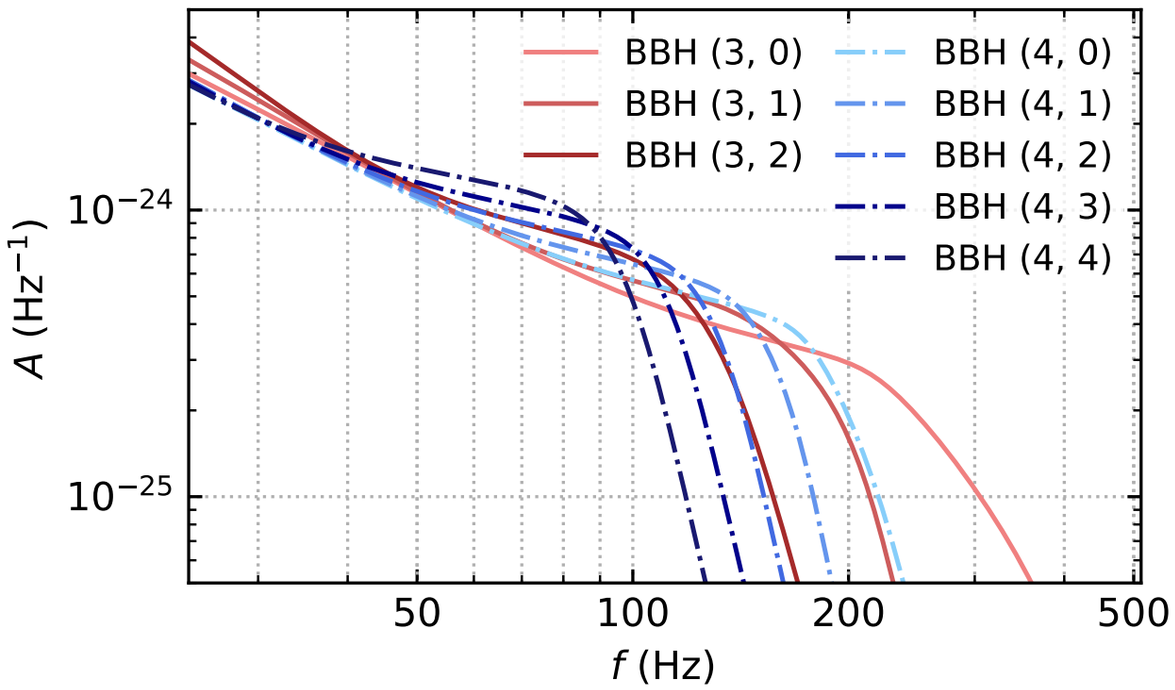

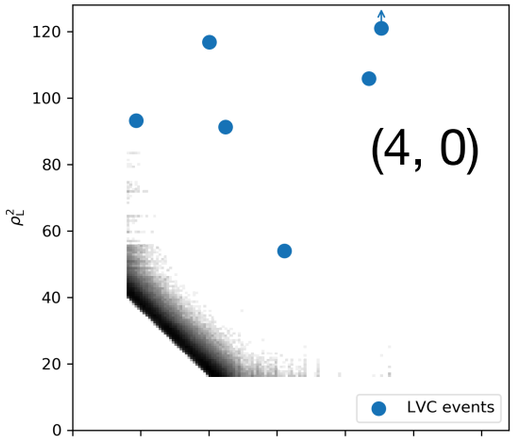

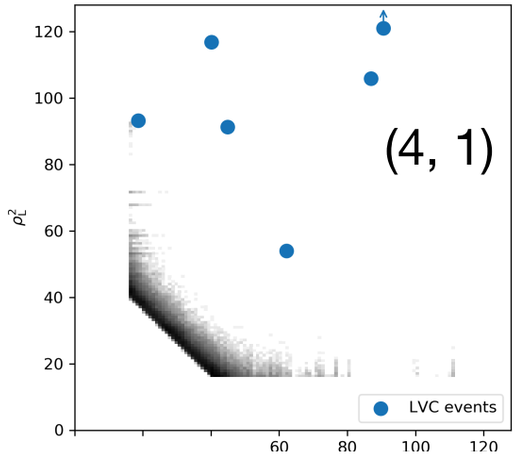

Vary with detector and parameters

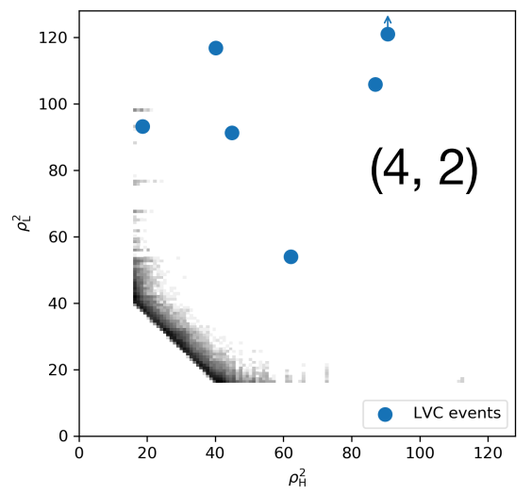

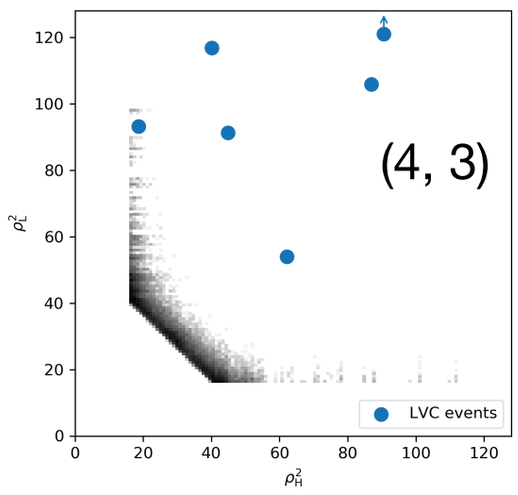

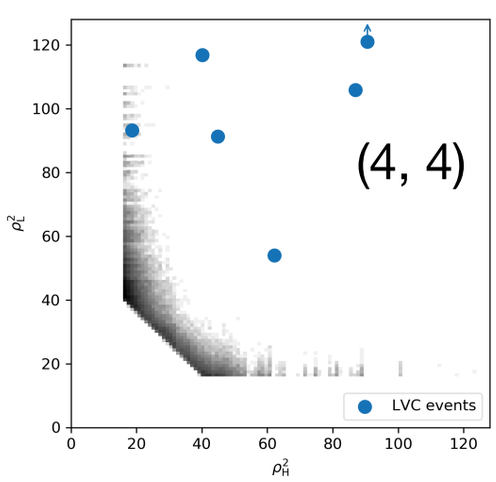

Tejaswi Venumadhav

Candidate lists (O3)

Name	Inst.	MBTA			GstLAL			PyCBC			PyCBC-BBH		
		FAR (yr^{-1})	SNR	p_{astro}	FAR (yr^{-1})	SNR	p_{astro}	FAR (yr^{-1})	SNR	p_{astro}	FAR (yr^{-1})	SNR	p_{astro}
GW190403_051519	HL	––	––	––	––	––	––	––	––	––	7.7	8.0	0.61
GW190408_181802	HLV	8.7×10^{-5}	14.4	1.00	$< 1.0 \times 10^{-5}$	14.7	1.00	2.5×10^{-4}	13.1	1.00	$< 1.2 \times 10^{-4}$	13.7	1.00
GW190412	HLV	$< 1.0 \times 10^{-5}$	18.2	1.00	$< 1.0 \times 10^{-5}$	19.0	1.00	$< 1.1 \times 10^{-4}$	17.4	1.00	$< 1.2 \times 10^{-4}$	17.9	1.00
GW190413_052954	HL	––	––	––	––	––	––	*170*	*8.5*	*0.13*	0.82	8.5	0.93
GW190413_134308	HLV	0.34	10.3	0.99	*39*	*10.1*	*0.04*	*21*	*9.3*	*0.48*	0.18	8.9	0.99
GW190421_213856	HL	1.2	9.7	0.99	0.0028	10.5	1.00	5.9	10.1	0.75	0.014	10.1	1.00
GW190425	LV	––	––	––	$0.034^{\dagger}$	12.9	0.78	––	––	––	––	––	––
GW190426_190642	HL	––	––	––	––	––	––	––	––	––	4.1	9.6	0.75
GW190503_185404	HLV	0.013	12.8	1.00	$< 1.0 \times 10^{-5}$	12.0	1.00	0.038	12.2	1.00	0.0026	12.2	1.00
GW190512_180714	HLV	0.038	11.7	0.99	$< 1.0 \times 10^{-5}$	12.2	1.00	1.1×10^{-4}	12.4	1.00	$< 1.1 \times 10^{-4}$	12.4	1.00
GW190513_205428	HLV	0.11	13.0	0.99	1.3×10^{-5}	12.3	1.00	*19*	*11.6*	*0.49*	0.044	11.8	1.00
GW190514_065416	HL	––	––	––	*450*	*8.3*	*0.00*	––	––	––	2.8	8.4	0.76
GW190517_055101	HLV	0.11	11.3	1.00	0.0045	10.8	1.00	0.0095	10.4	1.00	3.5×10^{-4}	10.3	1.00
GW190519_153544	HLV	7.0×10^{-5}	13.7	1.00	$< 1.0 \times 10^{-5}$	12.4	1.00	$< 1.0 \times 10^{-4}$	13.2	1.00	$< 1.1 \times 10^{-4}$	13.2	1.00
GW190521	HLV	0.042	13.0	0.96	0.20	13.3	0.79	0.44	13.7	0.96	0.0013	13.6	1.00
GW190521_074359	HL	$< 1.0 \times 10^{-5}$	22.2	1.00	$< 1.0 \times 10^{-5}$	24.4	1.00	$< 1.8 \times 10^{-5}$	24.0	1.00	$< 2.3 \times 10^{-5}$	24.0	1.00
GW190527_092055	HL	––	––	––	0.23	8.7	0.85	––	––	––	*19*	*8.4*	*0.33*
GW190602_175927	HLV	3.0×10^{-4}	12.6	1.00	$< 1.0 \times 10^{-5}$	12.3	1.00	0.29	11.9	0.98	0.013	11.9	1.00
GW190620_030421	LV	––	––	––	$0.011^{\dagger}$	10.9	0.99	––	––	––	––	––	––
GW190630_185205	LV	––	––	––	$< 1.0 \times 10^{-5}$	15.2	1.00	––	––	––	0.24	15.1	1.00
GW190701_203306	HLV	35	11.3	0.87	0.0057	11.7	0.99	0.064	11.9	0.99	0.56	11.7	1.00
GW190706_222641	HLV	0.0015	11.9	1.00	5.0×10^{-5}	12.5	1.00	3.7×10^{-4}	11.7	1.00	0.34	12.6	1.00
GW190707_093326	HL	0.032	12.6	1.00	$< 1.0 \times 10^{-5}$	13.2	1.00	$< 1.0 \times 10^{-5}$	13.0	1.00	$< 1.9 \times 10^{-5}$	13.0	1.00
GW190708_232457	LV	––	––	––	$3.1 \times 10^{-4\dagger}$	13.1	1.00	––	––	––	––	––	––
GW190719_215514	HL	––	––	––	––	––	––	––	––	––	0.63	8.0	0.92
GW190720_000836	HLV	0.094	11.6	1.00	$< 1.0 \times 10^{-5}$	11.5	1.00	1.4×10^{-4}	10.6	1.00	$< 7.8 \times 10^{-5}$	11.4	1.00
GW190725_174728*	HLV	3.1	9.8	0.59	––	––	––	0.46	9.1	0.96	2.9	8.8	0.82
GW190727_060333	HLV	0.023	12.0	1.00	$< 1.0 \times 10^{-5}$	12.1	1.00	0.0056	11.4	1.00	2.0×10^{-4}	11.1	1.00
GW190728_064510	HLV	7.5×10^{-4}	13.1	1.00	$< 1.0 \times 10^{-5}$	13.4	1.00	$< 8.2 \times 10^{-5}$	13.0	1.00	$< 7.8 \times 10^{-5}$	13.0	1.00
GW190731_140936	HL	6.1	9.1	0.80	0.33	8.5	0.78	––	––	––	1.9	7.8	0.83
GW190803_022701	HLV	77	9.0	0.96	0.073	9.1	0.94	*81*	*8.7*	*0.17*	0.39	8.7	0.97
GW190805_211137	HL	––	––	––	––	––	––	––	––	––	0.63	8.3	0.95
GW190814	LV	$< 2.0 \times 10^{-4}$	20.4	1.00	$< 1.0 \times 10^{-5}$	22.2	1.00	0.17	19.5	1.00	––	––	––
GW190828_063405	HLV	$< 1.0 \times 10^{-5}$	15.2	1.00	$< 1.0 \times 10^{-5}$	16.3	1.00	$< 8.5 \times 10^{-5}$	13.9	1.00	$< 7.0 \times 10^{-5}$	15.9	1.00
GW190828_065509	HLV	0.16	10.8	0.96	3.5×10^{-5}	11.1	1.00	2.8×10^{-4}	10.5	1.00	1.1×10^{-4}	10.5	1.00
GW190910_112807	LV	––	––	––	$0.0029^{\dagger}$	13.4	1.00	––	––	––	––	––	––
GW190915_235702	HLV	0.0055	12.7	1.00	$< 1.0 \times 10^{-5}$	13.0	1.00	6.8×10^{-4}	13.0	1.00	$< 7.0 \times 10^{-5}$	13.1	1.00
GW190916_200658*	HLV	6.9×10^{3}	8.2	0.66	*12*	*8.2*	*0.09*	––	––	––	4.7	7.9	0.64
GW190917_114630	HLV	––	––	––	0.66	9.5	0.77	––	––	––	––	––	––
GW190924_021846	HLV	0.0049	11.9	0.99	$< 1.0 \times 10^{-5}$	13.0	1.00	$< 8.2 \times 10^{-5}$	12.4	1.00	8.3×10^{-5}	12.5	1.00
GW190925_232845*	HV	*100*	*9.4*	*0.35*	––	––	––	*73*	*9.0*	*0.02*	0.0072	9.9	0.99
GW190926_050336*	HLV	––	––	––	1.1	9.0	0.54	––	––	––	*87*	*7.8*	*0.09*
GW190929_012149	HLV	2.9	10.3	0.64	0.16	10.1	0.87	*120*	*9.4*	*0.14*	*14*	*8.5*	*0.41*
GW190930_133541	HL	0.34	10.0	0.87	0.43	10.1	0.76	0.018	9.8	1.00	0.012	10.0	1.00

Name	Inst.	cWB			GstLAL			MBTA			PyCBC-broad			PyCBC-BBH		
		FAR (yr^{-1})	SNR	p_{astro}	FAR (yr^{-1})	SNR	p_{astro}	FAR (yr^{-1})	SNR	p_{astro}	FAR (yr^{-1})	SNR	p_{astro}	FAR (yr^{-1})	SNR	p_{astro}
GW191103_012549	HL	–	–	–	–	–	–	*27*	*9.0*	*0.13*	4.8	9.3	0.77	0.46	9.3	0.94
GW191105_143521	HLV	–	–	–	*24*	*10.0*	*0.07*	0.14	10.7	> 0.99	0.012	9.8	> 0.99	0.036	9.8	> 0.99
GW191109_010717	HL	< 0.0011	15.6	> 0.99	0.0010	15.8	> 0.99	1.8×10^{-4}	15.2	> 0.99	0.096	13.2	> 0.99	0.047	14.4	> 0.99
GW191113_071753	HLV	–	–	–	–	–	–	26	9.2	0.68	*1.1×10^{4}*	*8.3*	*< 0.01*	*1.2×10^{3}*	*8.5*	*< 0.01*
GW191126_115259	HL	–	–	–	*80*	*8.7*	*0.02*	*59*	*8.5*	*0.30*	*22*	*8.5*	*0.39*	3.2	8.5	0.70
GW191127_050227	HLV	–	–	–	*0.25*	*10.3*	*0.49*	1.2	9.8	0.73	*20*	*9.5*	*0.47*	4.1	8.7	0.74
GW191129_134029	HL	–	–	–	$< 1.0 \times 10^{-5}$	13.3	> 0.99	0.013	12.7	> 0.99	$< 2.6 \times 10^{-5}$	12.9	> 0.99	$< 2.4 \times 10^{-5}$	12.9	> 0.99
GW191204_110529	HL	–	–	–	*21*	*9.0*	*0.07*	*1.3×10^{4}*	*8.1*	*< 0.01*	*980*	*8.9*	*< 0.01*	3.3	8.9	0.74
GW191204_171526	HL	$< 8.7 \times 10^{-4}$	17.1	> 0.99	$< 1.0 \times 10^{-5}$	15.6	> 0.99	$< 1.0 \times 10^{-5}$	17.1	> 0.99	$< 1.4 \times 10^{-5}$	16.9	> 0.99	$< 1.2 \times 10^{-5}$	16.9	> 0.99
GW191215_223052	HLV	0.12	9.8	0.95	$< 1.0 \times 10^{-5}$	10.9	> 0.99	0.22	10.8	> 0.99	0.0016	10.3	> 0.99	0.28	10.2	> 0.99
GW191216_213338	HV	–	–	–	$< 1.0 \times 10^{-5}$	18.6	> 0.99	9.3×10^{-4}	17.9	> 0.99	0.0019	18.3	> 0.99	7.6×10^{-4}	18.3	> 0.99
GW191219_163120	HLV	–	–	–	–	–	–	–	–	–	4.0	8.9	0.82	–	–	–
GW191222_033537	HL	$< 8.9 \times 10^{-4}$	11.1	> 0.99	$< 1.0 \times 10^{-5}$	12.0	> 0.99	0.0099	10.8	> 0.99	0.0021	11.5	> 0.99	9.8×10^{-5}	11.5	> 0.99
GW191230_180458	HLV	0.050	10.3	0.95	0.13	10.3	0.87	*8.1*	*9.8*	*0.40*	*52*	*9.6*	*0.29*	0.42	9.9	0.96
GW200112_155838	LV	–	–	–	$< 1.0 \times 10^{-5\dagger}$	17.6	> 0.99	–	–	–	–	–	–	–	–	–
GW200115_042309	HLV	–	–	–	$< 1.0 \times 10^{-5}$	11.5	> 0.99	0.0055	11.2	> 0.99	$< 1.2 \times 10^{-4}$	10.8	> 0.99	–	–	–
GW200128_022011	HL	1.3	8.8	0.63	0.022	10.1	0.97	3.3	9.4	0.98	0.63	9.8	0.95	0.0043	9.9	> 0.99
GW200129_065458	HLV	–	–	–	$< 1.0 \times 10^{-5}$	26.5	> 0.99	–	–	–	$< 2.3 \times 10^{-5}$	16.3	> 0.99	$< 1.7 \times 10^{-5}$	16.2	> 0.99
GW200202_154313	HLV	–	–	–	$< 1.0 \times 10^{-5}$	11.3	> 0.99	–	–	–	–	–	–	0.025	10.8	> 0.99
GW200208_130117	HLV	–	–	–	0.0096	10.7	0.99	0.46	10.4	> 0.99	0.18	9.6	0.98	3.1×10^{-4}	10.8	> 0.99
GW200208_222617	HLV	–	–	–	*160*	*8.2*	*< 0.01*	*420*	*8.9*	*0.02*	–	–	–	4.8	7.9	0.70
GW200209_085452	HLV	–	–	–	0.046	10.0	0.95	12	9.7	0.97	*550*	*9.2*	*0.04*	1.2	9.2	0.89
GW200210_092254	HLV	–	–	–	*1.2*	*9.5*	*0.42*	–	–	–	17	8.9	0.53	7.7	8.9	0.54
GW200216_220804	HLV	–	–	–	0.35	9.4	0.77	*2.4×10^{3}*	*8.8*	*0.02*	*970*	*9.0*	*< 0.01*	7.8	8.7	0.54
GW200219_094415	HLV	0.77	9.7	0.85	9.9×10^{-4}	10.7	> 0.99	0.18	10.6	> 0.99	1.7	9.9	0.89	0.016	10.0	> 0.99
GW200220_061928	HLV	–	–	–	–	–	–	–	–	–	–	–	–	6.8	7.5	0.62
GW200220_124850	HL	–	–	–	*150*	*8.2*	*< 0.01*	1.8×10^{3}	8.2	0.83	–	–	–	*30*	*7.8*	*0.20*
GW200224_222234	HLV	$< 8.8 \times 10^{-4}$	18.8	> 0.99	$< 1.0 \times 10^{-5}$	18.9	> 0.99	$< 1.0 \times 10^{-5}$	19.0	> 0.99	$< 8.2 \times 10^{-5}$	19.2	> 0.99	$< 7.7 \times 10^{-5}$	18.6	> 0.99
GW200225_060421	HL	$< 8.8 \times 10^{-4}$	13.1	> 0.99	0.079	12.9	0.93	0.0049	12.5	> 0.99	$< 1.1 \times 10^{-5}$	12.3	> 0.99	4.1×10^{-5}	12.3	> 0.99
GW200302_015811	HV	–	–	–	$0.11^{\dagger}$	10.6	0.91	–	–	–	–	–	–	–	–	–
GW200306_093714	HL	–	–	–	–	–	–	410	8.5	0.81	*3.4×10^{3}*	*7.8*	*< 0.01*	*24*	*8.0*	*0.24*
GW200308_173609	HLV	–	–	–	*680*	*8.1*	*< 0.01*	*6.9×10^{4}*	*8.3*	*0.24*	*770*	*7.9*	*< 0.01*	2.4	8.0	0.86
GW200311_115853	HLV	$< 8.2 \times 10^{-4}$	16.2	> 0.99	$< 1.0 \times 10^{-5}$	17.7	> 0.99	$< 1.0 \times 10^{-5}$	16.5	> 0.99	$< 6.9 \times 10^{-5}$	17.0	> 0.99	$< 7.7 \times 10^{-5}$	17.4	> 0.99
GW200316_215756	HLV	–	–	–	$< 1.0 \times 10^{-5}$	10.1	> 0.99	*12*	*9.5*	*0.30*	0.20	9.3	0.98	0.58	9.3	0.98
GW200322_091133	HLV	–	–	–	–	–	–	450	9.0	0.62	*1.4×10^{3}*	*8.0*	*< 0.01*	*140*	*7.7*	*0.08*

GWTC 2.1 (O3a)
arxiv: 2108.01045

Criteria:
FAR < 2 day^(-1)
p_astro > 0.5

GWTC 3 (O3b)
arxiv: 2111.03606

See also OGC analyses:
Nitz et. al. (2021)

Tejaswi Venumadhav

Our search

- Construct template banks
- Whiten and clean the data
- Generate triggers and correct for non-stationary noise
- Collect coincident triggers and veto remaining glitches
- Coherently analyze remaining coincident triggers

$$Z(h) = \sum_f \frac{d(f)h^\star(f)}{\sigma^2(f)}$$

Impact of improved noise modeling and vetoes

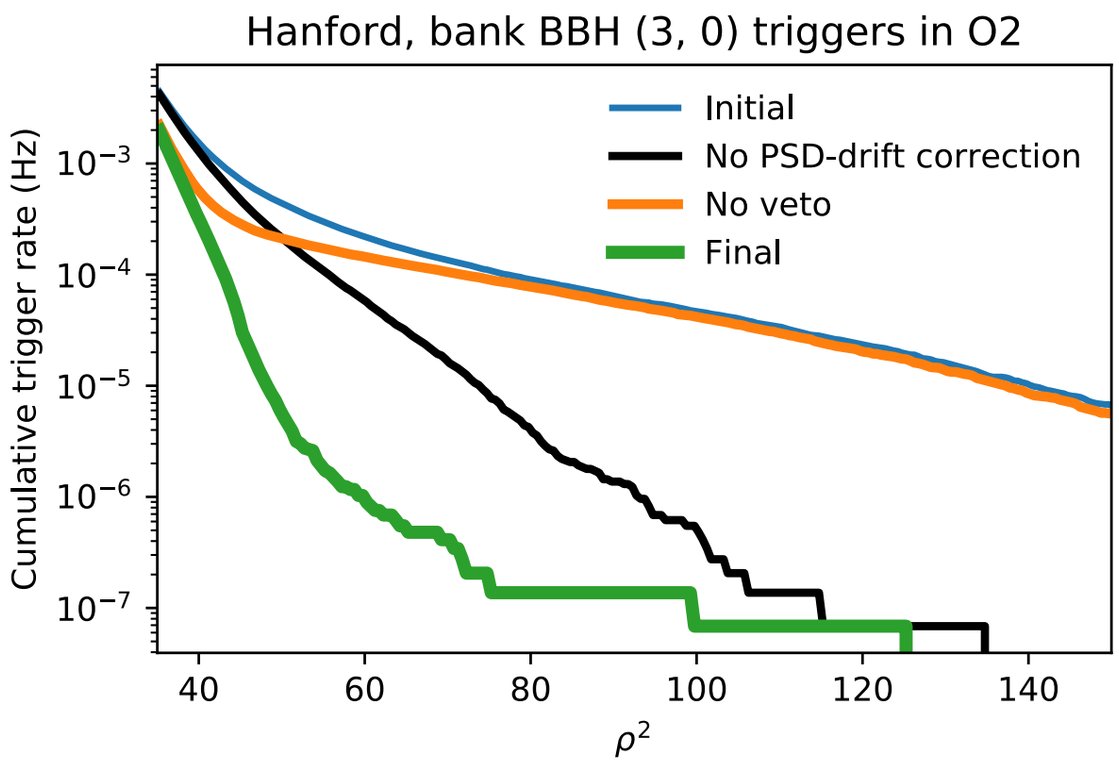

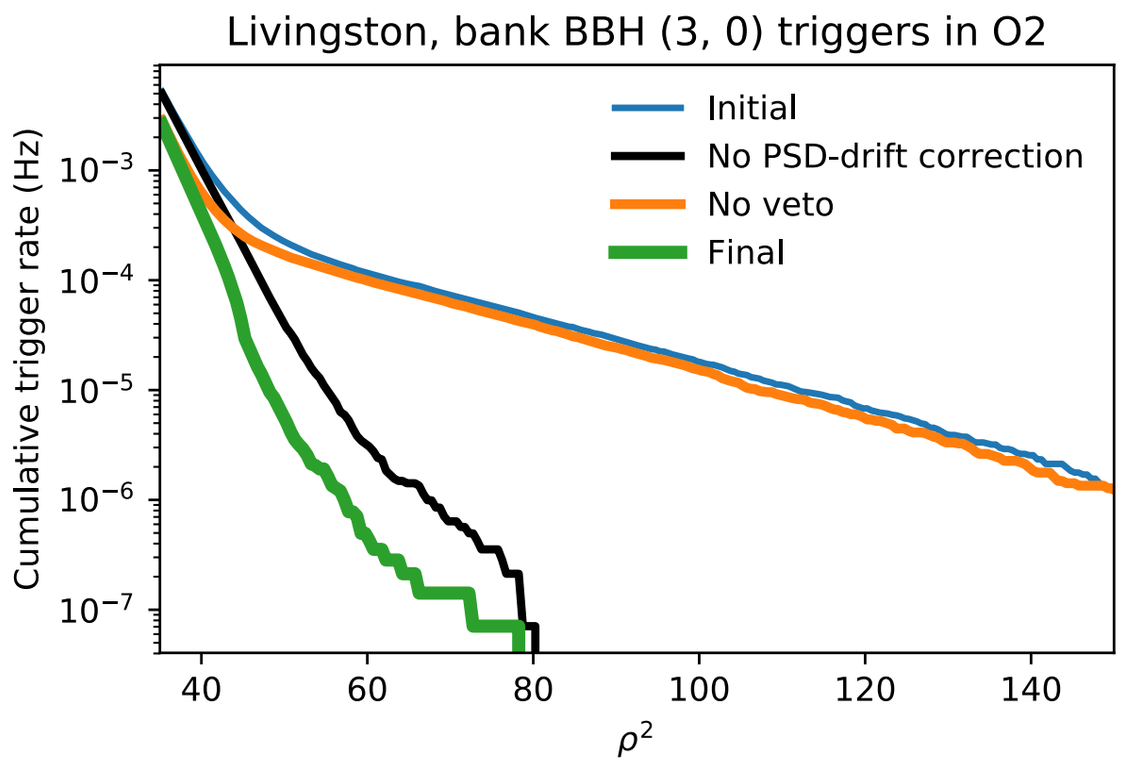

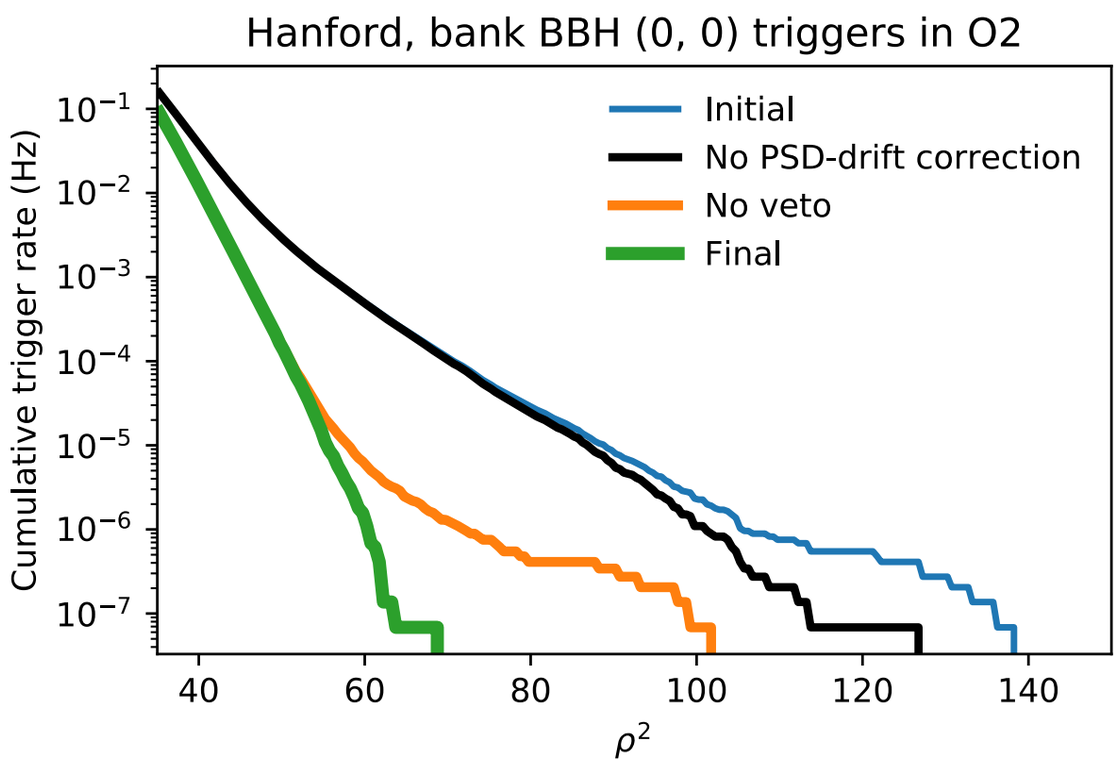

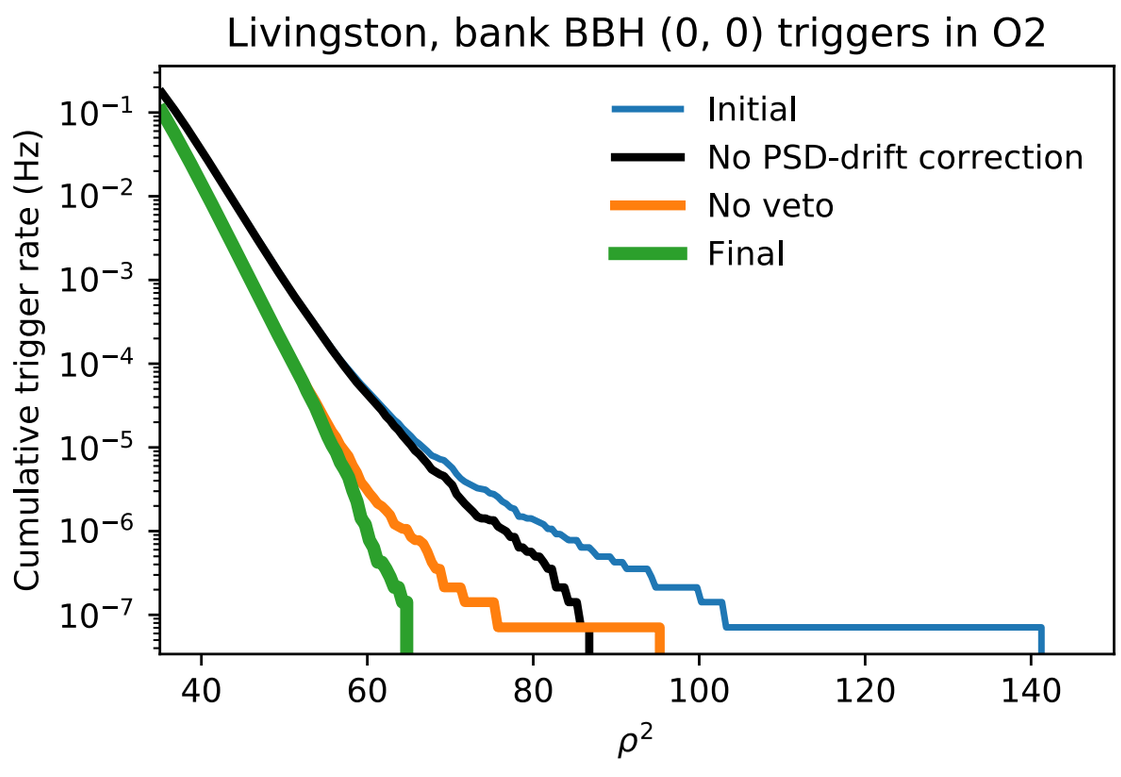

Zackay et. al., (2021)

Effect of mitigating glitches

$$z(h) = \sum_f \frac{d(f)h^\star(f)}{\sigma^2(f)}$$

Background

No vetoes

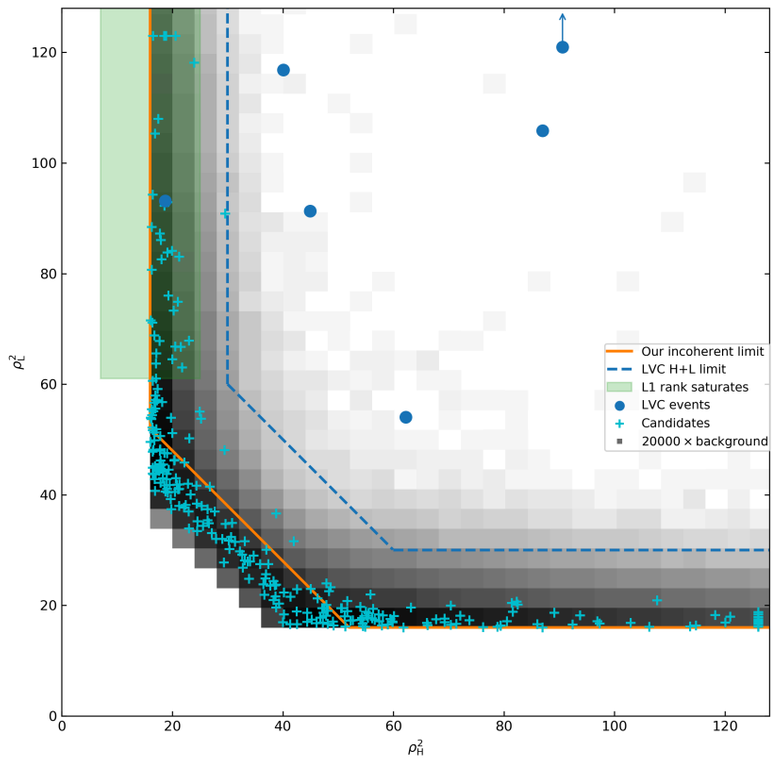

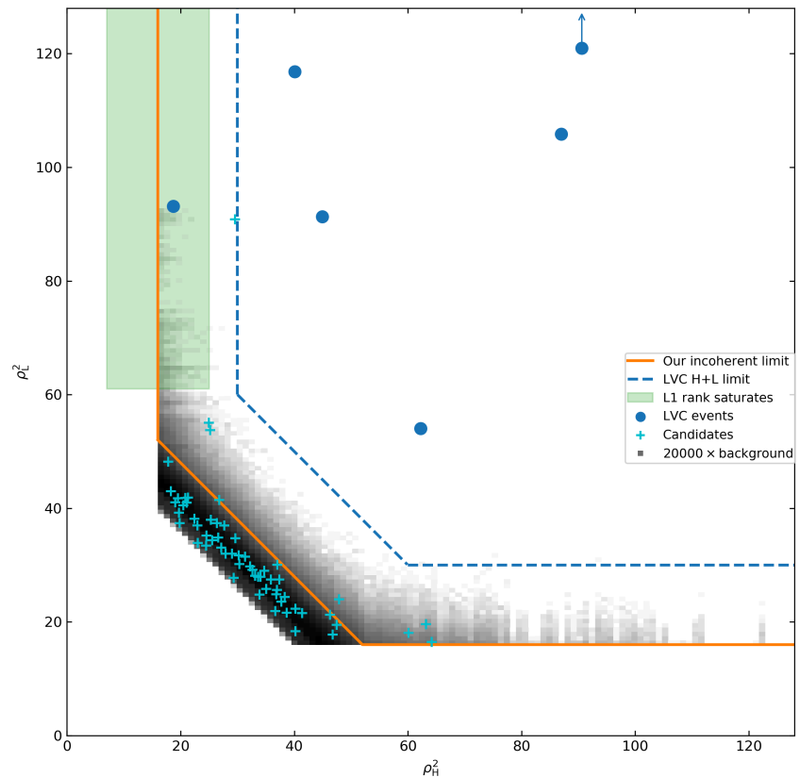

With vetoes

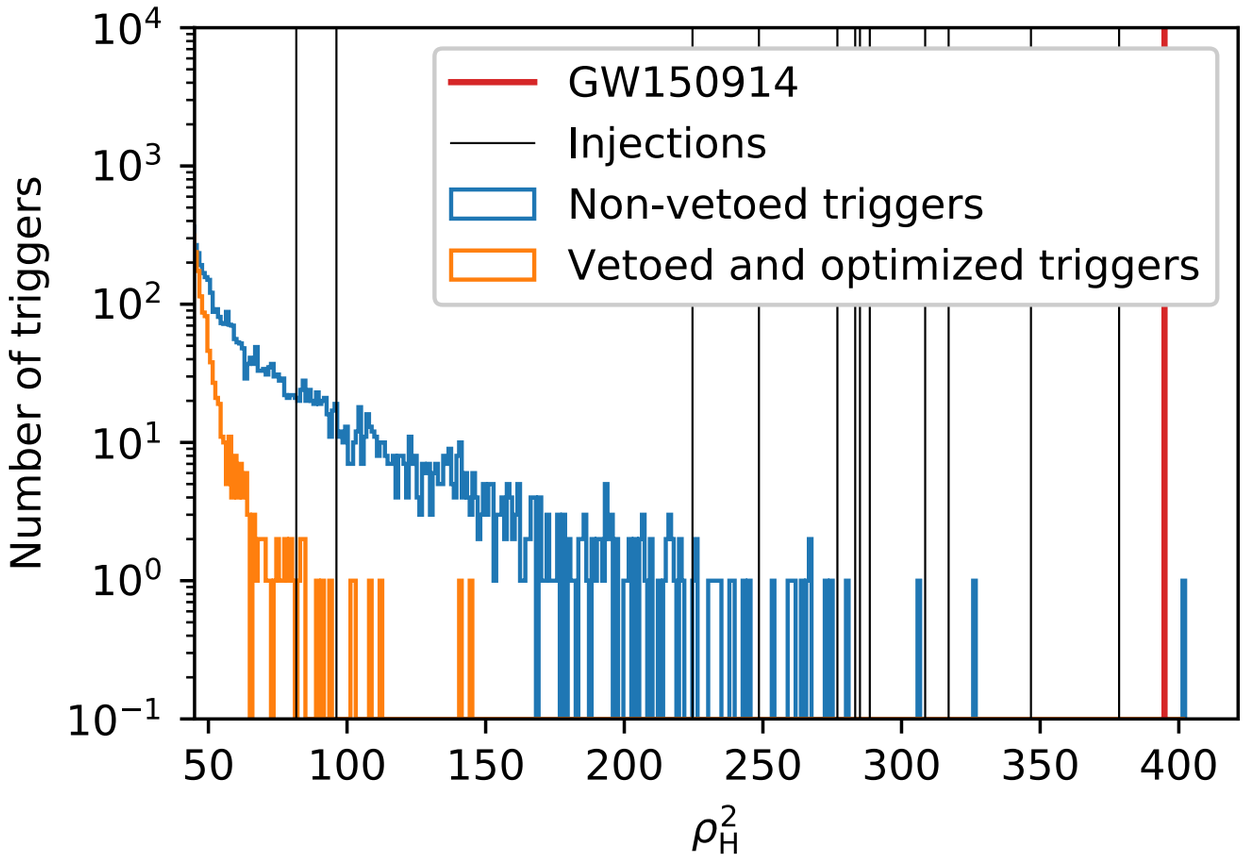

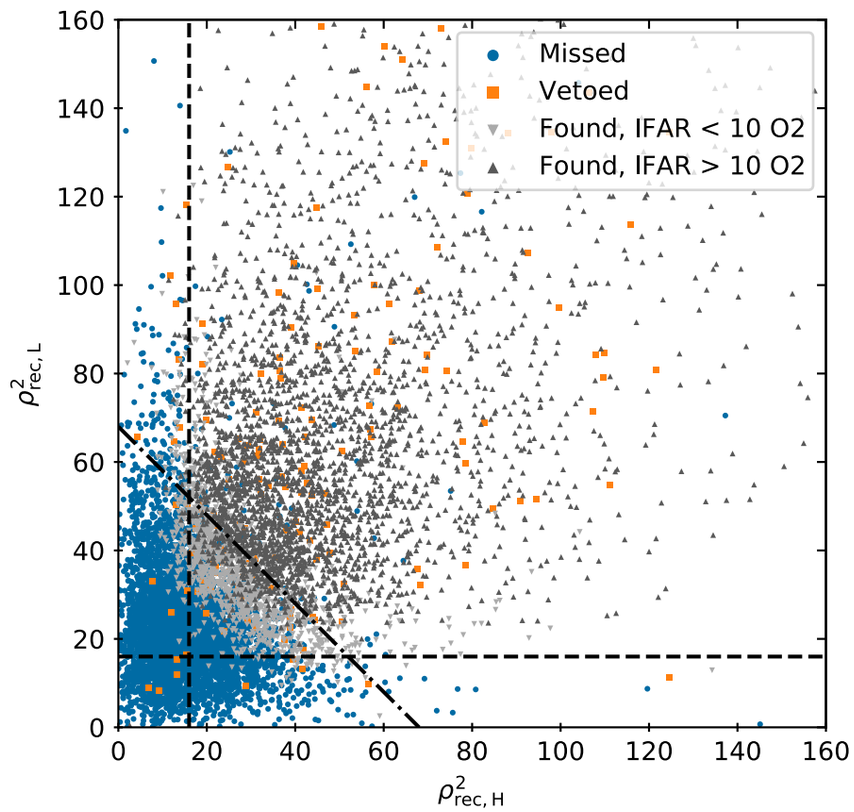

Injections

Roulet et. al., (2020)

Template Prior

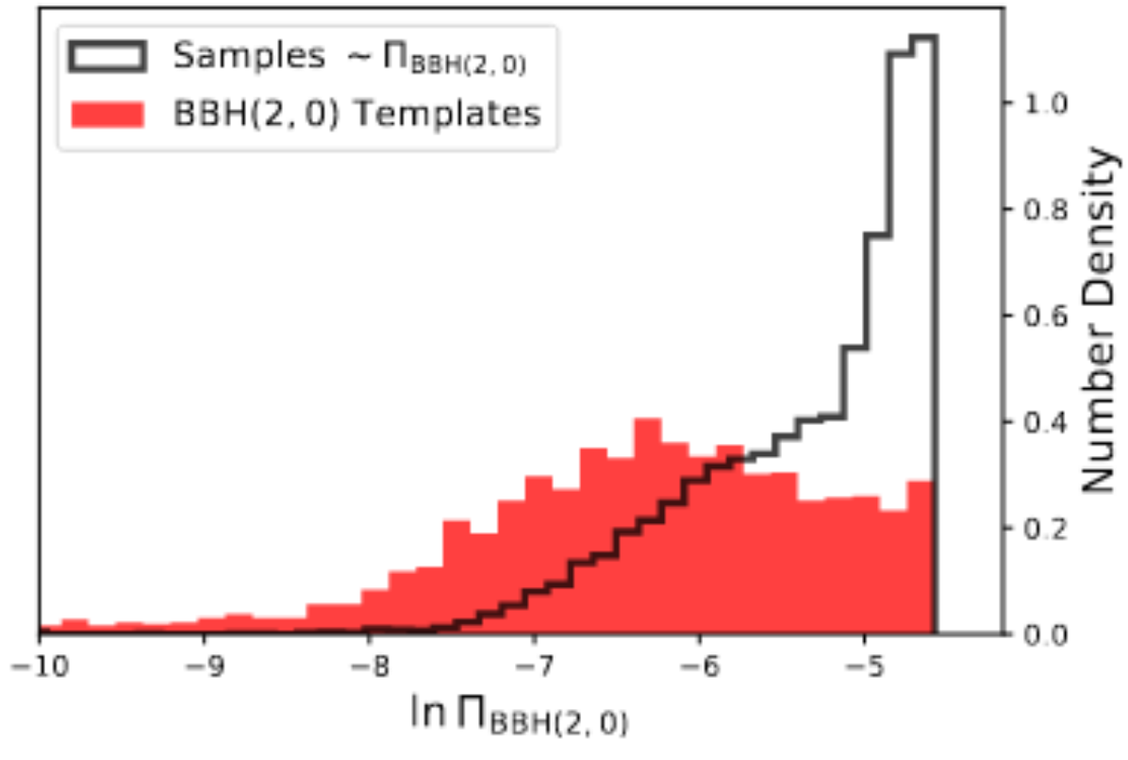

uniform c_α grid spacing over-represents regions of low prior relative to its coverage of the regions where physical templates are most likely. The template prior therefore decreases the impact of the look-elsewhere effect on the most physically probable regions of geometric grid space by raising the effective detection bar for templates in regions of grid space where the ratio of grid coordinate volume to physical parameter space volume is too large.

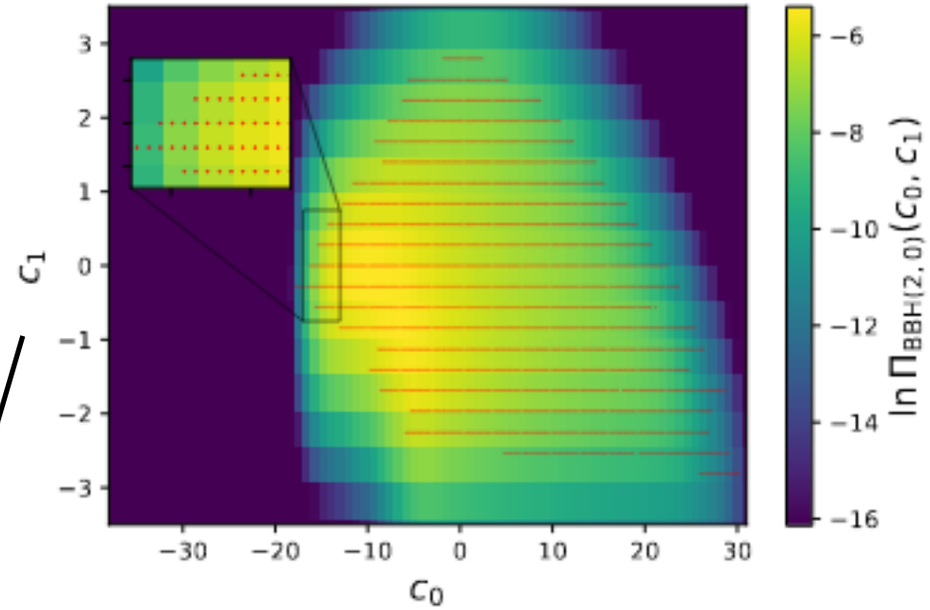

Π uniform in component masses and effective spin

Geometric coordinates

Olsen, S., TV, et. al. (2022)

See also Nitz et. al., (2017)

Multi-detector coherence

$$p(d|\mathcal{I}) = \int d\Pi(\mathcal{E}_m, \mathcal{E}_d) L(\mathcal{I}, \mathcal{E}_m, \mathcal{E}_d).$$

Prior

Likelihood

Extrinsic parameters:

- Inclination
- Orbital phase
- RA
- Dec
- Polarization angle
- Distance
- Merger time

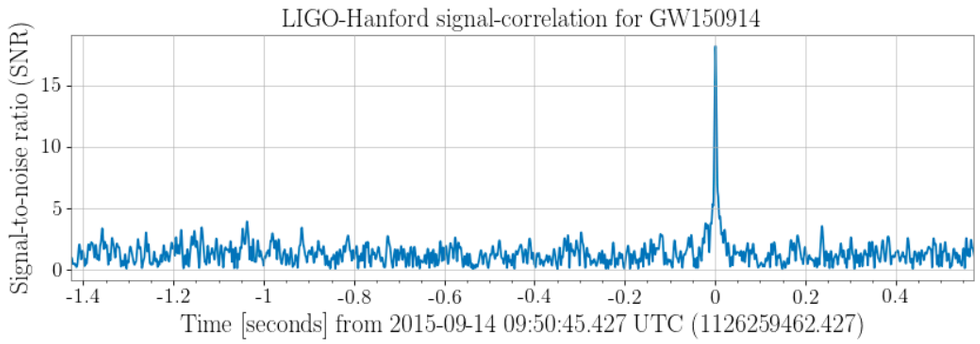

Credit: (GWpy)

$$\frac{p(d|\mathcal{I})}{p(d|\text{noise})} = \frac{4\pi\Pi_0 D_0^3}{T} \prod_{k\in \text{ detectors}} \int \mathrm{d}\tau_k \, \exp\left(\frac{1}{2}|Z_k(\tau_k)|^2\right) \int \frac{\mathrm{d}\alpha}{2\pi} \frac{\mathrm{d}\delta \cos\delta}{2} \, [\delta_{k,0} + (1-\delta_{k,0})\delta_{\mathrm{D}}(\Delta\tau_k - \Delta\tau_k(\alpha,\delta))] \times$$
$$\int \frac{\mathrm{d}\mu}{2} \frac{\mathrm{d}\psi}{2\pi} \, \exp\left\{-\frac{1}{2}\left(||\mathbf{Z}||^2 - |\hat{\mathbf{z}}_0(\mu,\alpha,\delta,\psi)\cdot\mathbf{Z}|^2\right)\right\} ||\mathbf{z}_0||^3 \, g(|\hat{\mathbf{z}}_0\cdot\mathbf{Z}|) \, . \qquad \text{(D82)}$$

Olsen, S., TV, et. al. (2022)

Candidate lists for O3a

Event Name	Bank	ρ_H^2	ρ_L^2	p_{astro}	IFAR (yr)		
					IAS[a]	GWTC-2.1	3-OGC
GW190403_051519	(4, 0)	23.1	29.7	—	Veto	0.13	—
GW190408_181802	(3, 0)	95.4	109.2	1.00	> 1000	> 1000	> 1000
GW190412_053044	(2, 0)	76.2	245.5	1.00	> 1000	> 1000	> 1000
GW190413_052954	(4, 0)	26.7	50.5	0.83	4.2	1.2	1.4
GW190413_134308	(4, 2)	30.1	62.3	1.00	> 1000	2.9	6.4
GW190421_213856	(4, 1)	68.0	42.0	1.00	> 1000	71.4	> 1000
GW190426_190642	(5, 5)	24.1	42.7	0.33	0.19	0.24	—
GW190503_185404	(3, 1)	83.2	57.7	1.00	> 1000	> 1000	> 1000
GW190512_180714	(2, 0)	39.4	119.4	1.00	> 1000	> 1000	> 1000
GW190513_205428	(3, 0)	78.0	66.0	1.00	> 1000	> 1000	> 1000
GW190514_065416	(4, 1)	38.9	31.7	0.98	290	0.36	0.19
GW190517_055101	(3, 1)	48.7	58.5	1.00	> 1000	9.1	66.1
GW190519_153544	(4, 2)	81.6	128.7	1.00	> 1000	> 1000	> 1000
GW190521_030229	(5, 5)	65.0	129.8	—	Veto	769	805
GW190521_074359	(3, 1)	142.3	431.3	1.00	> 1000	> 1000	> 1000
GW190527_092055	(3, 1)	27.4	46.9	0.92	10.8	4.3	0.37
GW190602_175927	(4, 3)	41.9	111.6	1.00	> 1000	> 1000	391
GW190701_203306	(2, 2)	25.1	53.8	0.23	0.084	1.8	0.13
GW190706_222641	(4, 3)	91.3	79.2	1.00	> 1000	2.9	> 1000
GW190707_093326	(1, 0)	63.7	97.5	1.00	> 1000	> 1000	> 1000
GW190719_215514	(3, 1)	37.0	33.2	0.90	8.5	1.6	0.25
GW190720_000836	(1, 0)	44.7	62.3	1.00	> 1000	10.6	559
GW190725_174728	(1, 0)	31.3	59.1	0.96	34.2	2.2	0.41
GW190727_060333	(4, 0)	76.0	61.3	1.00	> 1000	> 1000	> 1000
GW190728_064510	(1, 0)	58.4	110.1	1.00	> 1000	> 1000	> 1000
GW190731_140936	(3, 1)	28.9	39.6	0.76	2.1	0.53	0.43
GW190803_022701	(3, 1)	30.6	43.7	0.94	15.7	2.6	2.4
GW190805_211137	(4, 1)	18.8	54.8	0.81	3.3	1.6	—
GW190828_063405	(3, 1)	112.6	142.3	1.00	> 1000	> 1000	> 1000
GW190828_065509	(2, 1)	54.5	53.6	1.00	> 1000	> 1000	> 1000
GW190909_114149[b]	(3, 1)	31.3	32.4	0.52	0.45	0.010	—
GW190915_235702	(3, 0)	92.4	71.1	1.00	> 1000	> 1000	> 1000
GW190916_200658	(4, 2)	27.1	36.5	0.93	20.7	< 0.001	0.22
GW190917_114629	(0, 0)	26.8	40.6	0.35	0.17	1.5	—
GW190924_021846	(1, 0)	31.9	94.9	—	Veto	> 1000	> 1000
GW190926_050336	(3, 1)	45.3	31.4	0.96	25.3	0.91	0.27
GW190929_012149	(5, 2)	40.2	51.2	1.00	> 1000	6.2	3.1
GW190930_133541	(1, 0)	41.1	55.6	1.00	> 1000	55.6	295

New candidates

Name	Bank	$m_{1(M_\odot)}$	$m_{2(M_\odot)}$	χ_{eff}	z	$\ln \mathcal{L}_{max}$	ρ_H^2	ρ_L^2	IFAR (yr)[a]	p_{astro}
GW190707_083226	(4, 2)	52^{+17}_{-12}	32^{+12}_{-11}	$-0.2^{+0.5}_{-0.6}$	$0.6^{+0.4}_{-0.3}$	43.9	37.0	31.5	23.2	0.94
GW190711_030756	(3, 1)	80^{+50}_{-40}	18^{+11}_{-7}	$0.2^{+0.3}_{-0.7}$	$0.41^{+0.24}_{-0.16}$	49.5	19.8	60.7	11.2	0.93
GW190818_232544	(4, 3)	67^{+23}_{-19}	38^{+17}_{-15}	$0.7^{+0.2}_{-0.3}$	$1.0^{+0.6}_{-0.4}$	40.5*	33.0	32.0	3.4	0.81
GW190704_104834	(0, 0)	7^{+6}_{-2}	$3.2^{+1.2}_{-1.1}$	$0.20^{+0.27}_{-0.14}$	$0.10^{+0.03}_{-0.03}$	48.7*	47.0	32.1	2.8	0.81
GW190906_054335	(3, 1)	37^{+12}_{-8}	24^{+8}_{-8}	$0.1^{+0.4}_{-0.5}$	$0.9^{+0.4}_{-0.3}$	34.1*	23.6	38.1	0.73	0.61
GW190821_124821	(1, 0)	$7.6^{+3.9}_{-1.7}$	$4.0^{+1.0}_{-1.1}$	$-0.45^{+0.33}_{-0.17}$	$0.17^{+0.06}_{-0.06}$	48.5*	28.1	49.4	0.71	0.60
GW190814_192009	(5, 4)	68^{+28}_{-19}	48^{+21}_{-18}	$0.5^{+0.4}_{-0.6}$	$1.5^{+0.8}_{-0.7}$	25.2	29.9	33.4	0.65	0.64
GW190910_012619	(1, 1)	34^{+3}_{-3}	$2.9^{+0.3}_{-0.2}$	$-0.87^{+0.19}_{-0.11}$	$0.16^{+0.04}_{-0.04}$	40.2*	35.7	32.1	0.65	0.58
GW190920_113516	(0, 0)	$6.0^{+3.3}_{-1.5}$	$3.2^{+0.9}_{-1.0}$	$0.60^{+0.26}_{-0.07}$	$0.13^{+0.05}_{-0.05}$	40.7	26.4	48.0	0.56	0.57
GW190718_160159	(1, 0)	$10.0^{+4.5}_{-1.8}$	$6.8^{+1.4}_{-2.1}$	$0.73^{+0.10}_{-0.17}$	$0.28^{+0.10}_{-0.09}$	41.1*	23.5	47.6	0.48	0.53

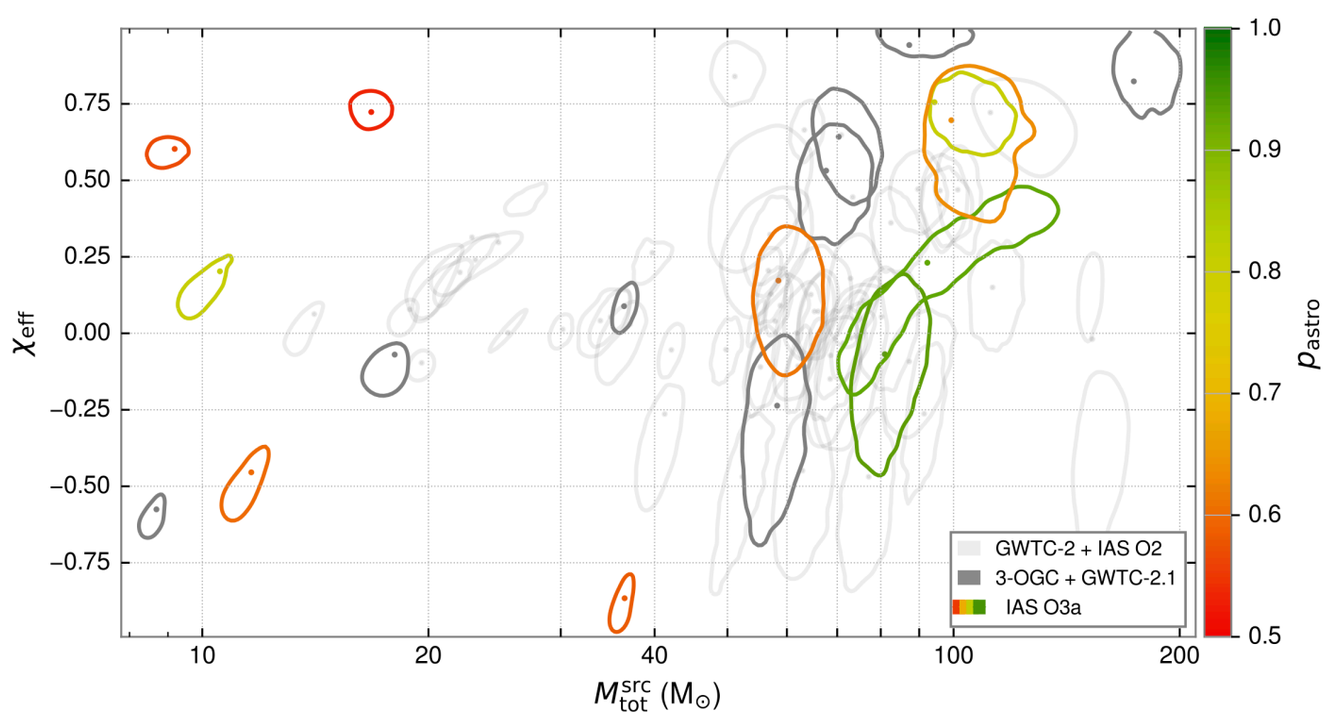

Results on known candidates

Interesting new events

- Signals with higher harmonics and orbital precession

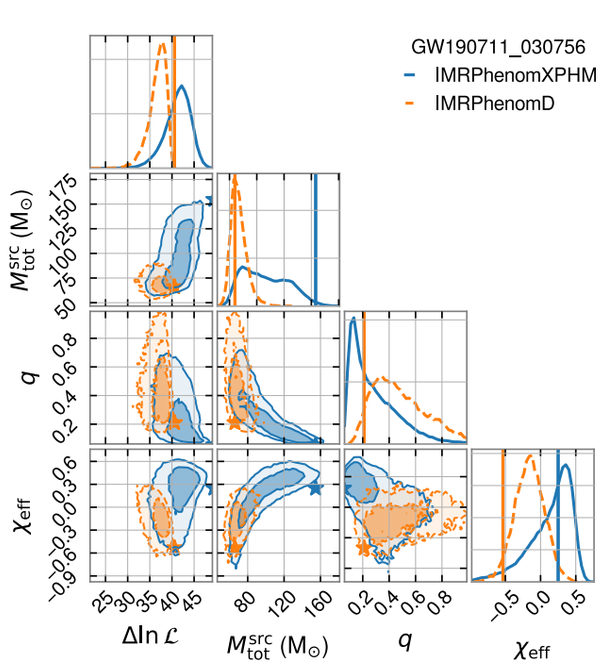

(a) Comoving Posteriors

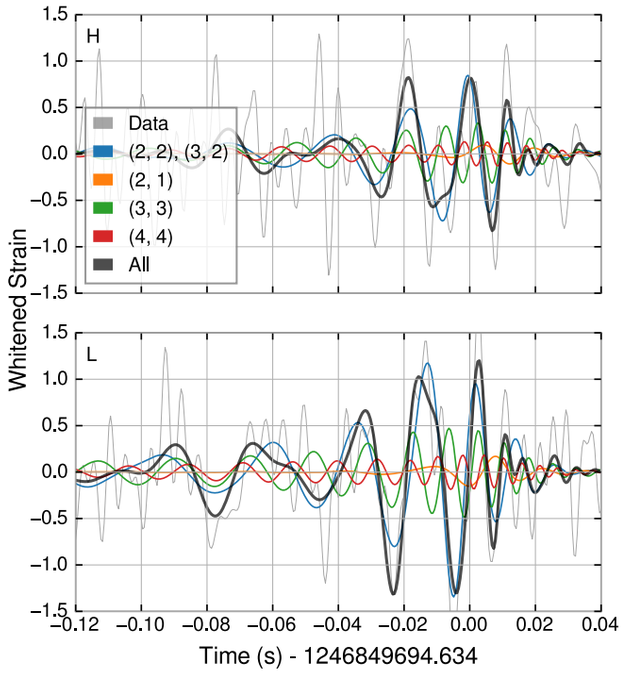

(b) Multipole Mode Content

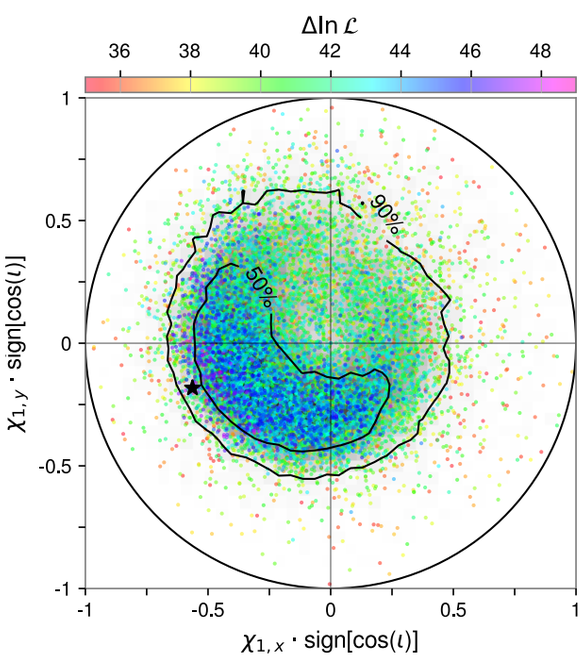

(c) In-Plane Spin

GW190711_030756 (p_astro = 0.93)

Interesting new events

- Events with BH masses in the lower and upper mass gaps

GW190704_104834: IFAR = 2.8 (y)

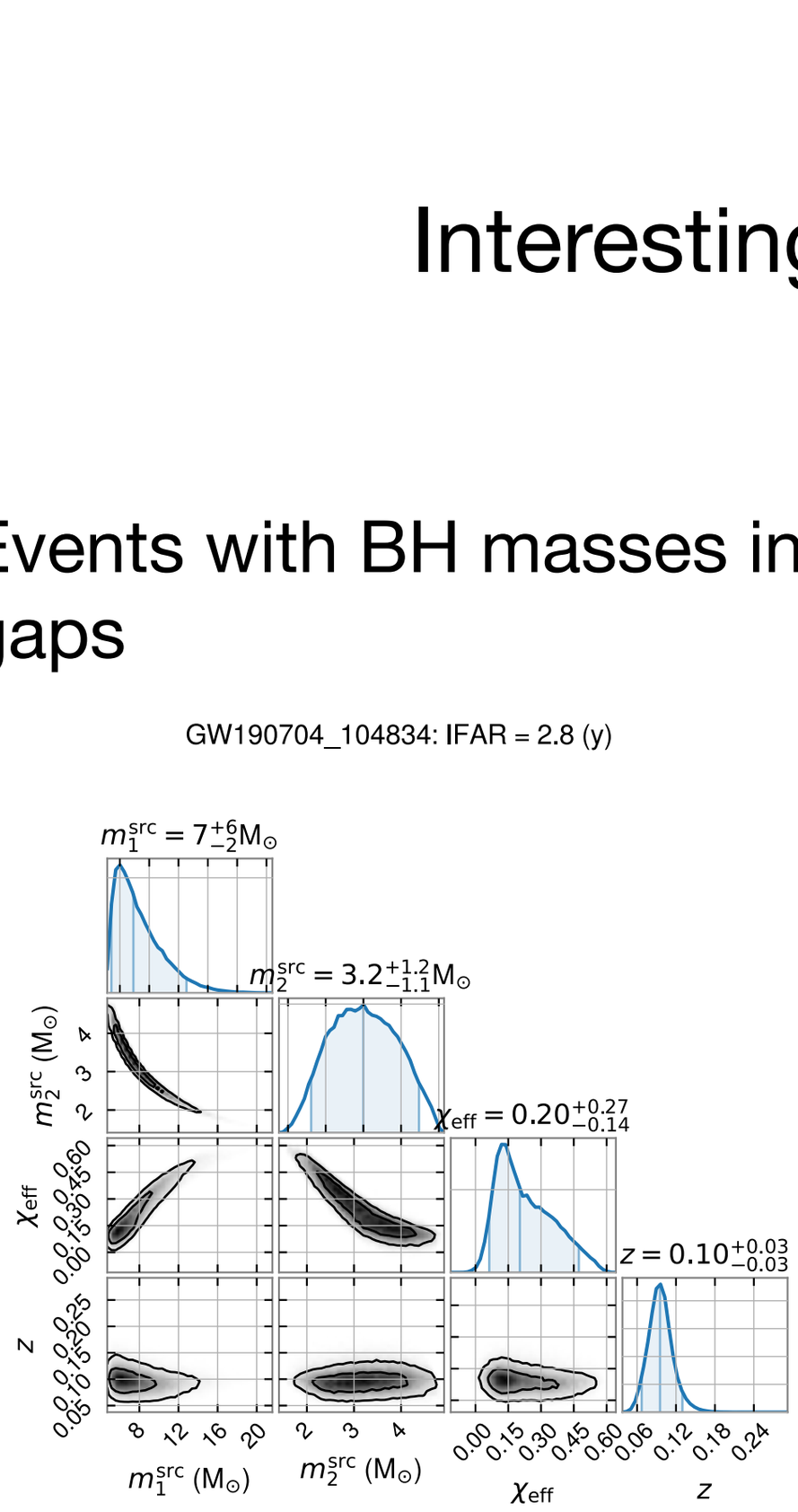

GW190818_232544: IFAR = 3.4 (y)

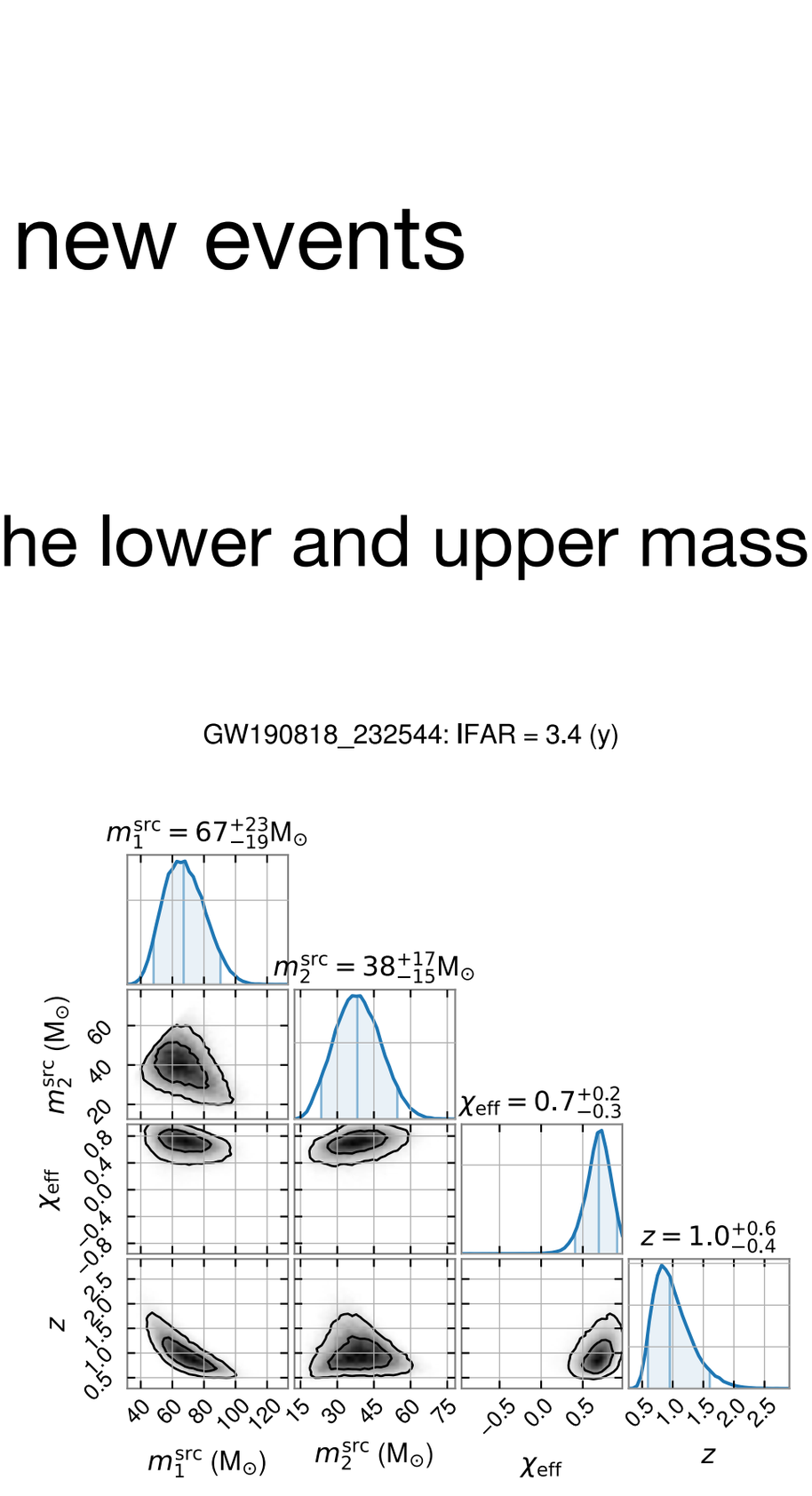

Population analysis

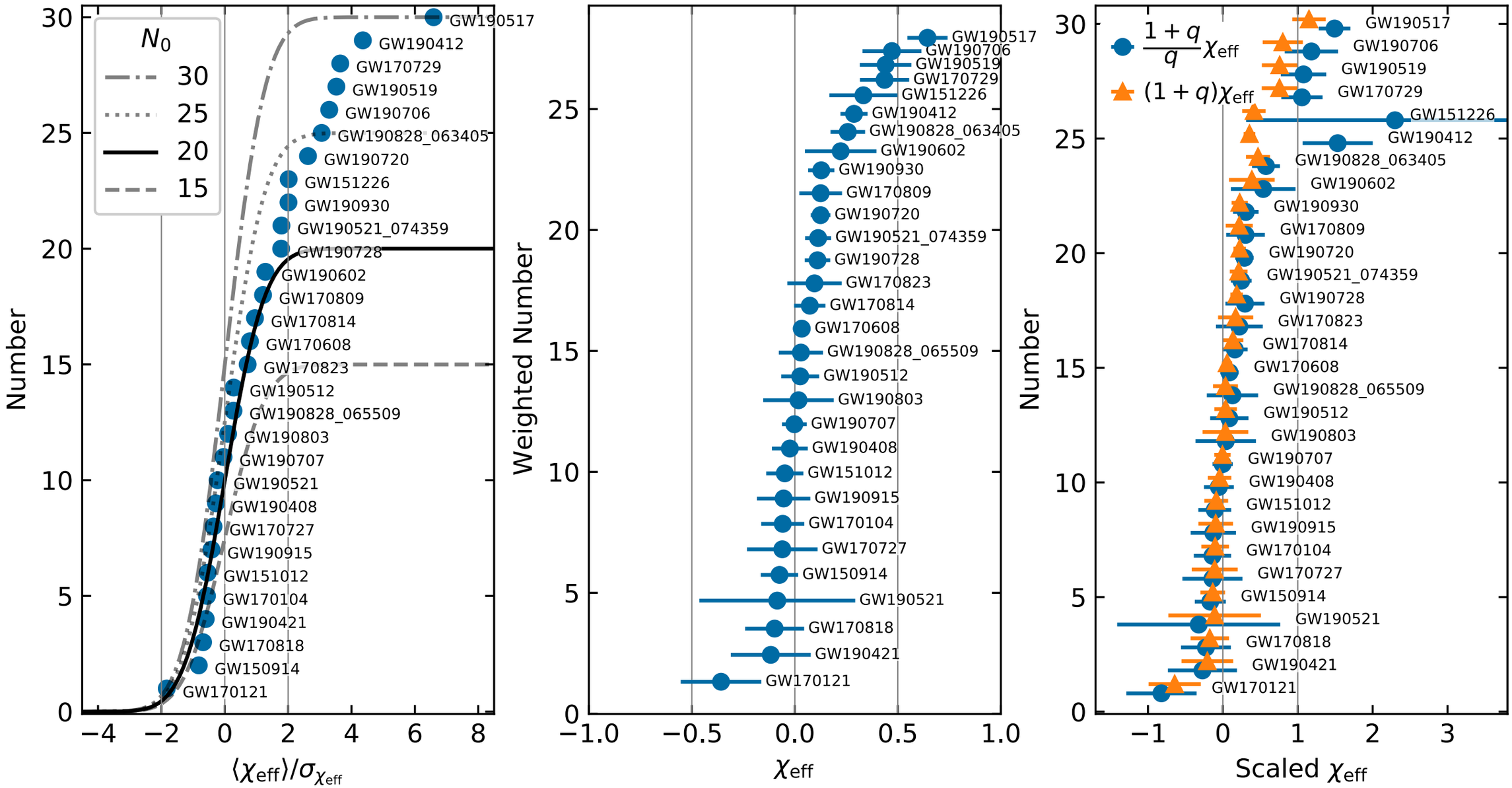

Puzzle in the distribution of the effective spin

$$\chi_{\rm eff} := \frac{\boldsymbol{\chi_1} + q\boldsymbol{\chi_2}}{1+q} \cdot \hat{\boldsymbol{L}},$$

Roulet et. al., (2021)

Population analysis

$$P(\{d_i\} \mid \lambda) \propto e^{-N_a(\lambda)} \prod_{i=1}^{N_{\rm trig}} \left(\left. \frac{\mathrm{d}N_a(\lambda)}{\mathrm{d}N_a(\lambda_0)} \right|_{d_i} p_{{\rm astro},i}(\lambda_0) + 1 - p_{{\rm astro},i}(\lambda_0) \right).$$

(Unknown) True model for BBH population

Fiducial model for BBH population

$$f(\chi_{\rm eff}, m_{1\rm s}, q, D_L) = f_{\chi_{\rm eff}}(\chi_{\rm eff}) f_{m_{1\rm s}}(m_{1\rm s}) f_q(q) f_{D_L}(D_L).$$

$$\begin{aligned} f_{\chi_{\rm eff}}(\chi_{\rm eff} \mid \zeta_{\rm pos}, \zeta_{\rm neg}, \sigma_{\chi_{\rm eff}}) = \zeta_0 \mathcal{N}(\chi_{\rm eff}; \sigma_0 = 0.04) \\ + \zeta_{\rm neg} \mathcal{N}_{<0}(\chi_{\rm eff}; \sigma_{\chi_{\rm eff}}) \\ + \zeta_{\rm pos} \mathcal{N}_{>0}(\chi_{\rm eff}; \sigma_{\chi_{\rm eff}}) \, . \end{aligned}$$

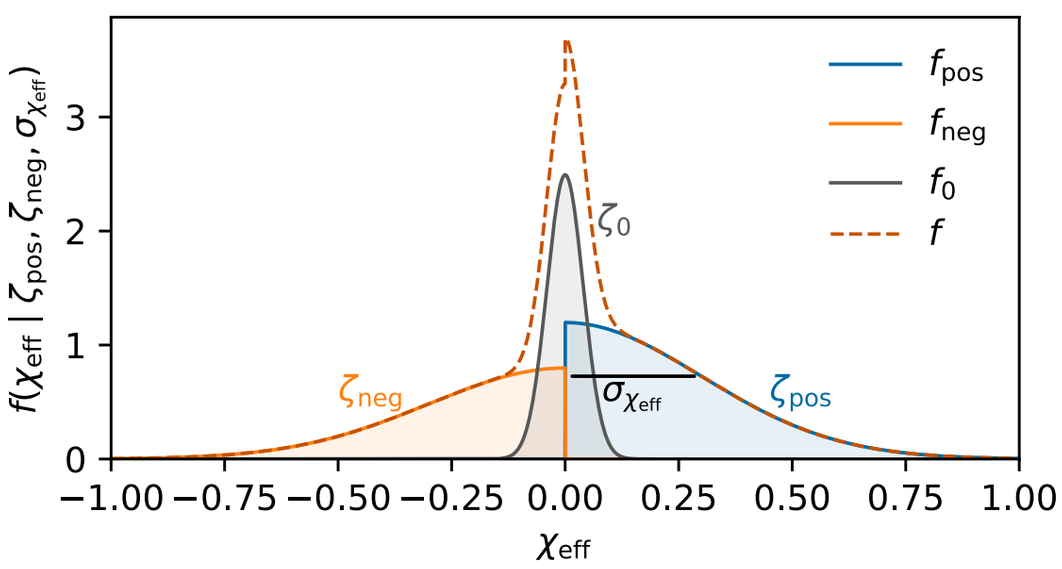

Roulet et. al., (2020, 2021)

Population analysis

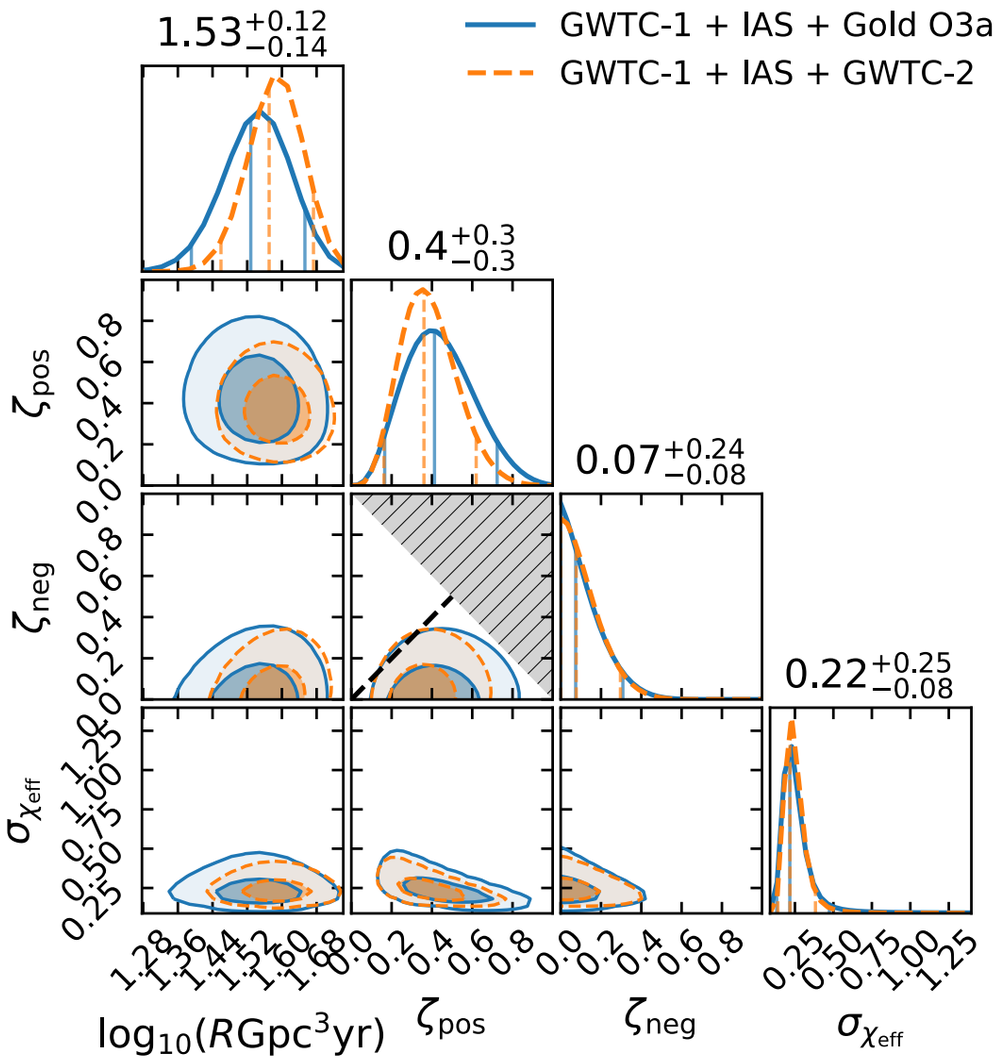

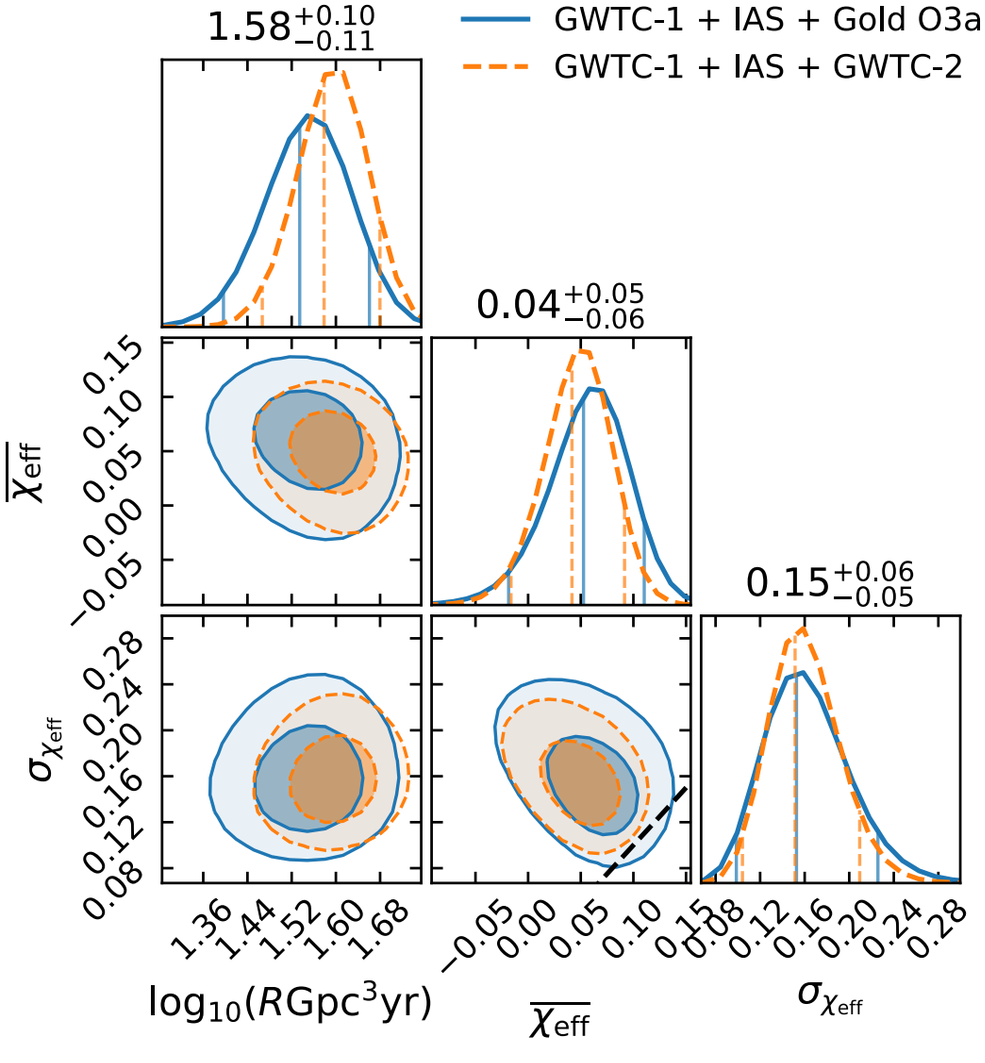

$$f_{\chi_{\rm eff}}(\chi_{\rm eff} \mid \zeta_{\rm pos}, \zeta_{\rm neg}, \sigma_{\chi_{\rm eff}}) = \zeta_0 \mathcal{N}(\chi_{\rm eff}; \sigma_0 = 0.04) + \zeta_{\rm neg}\mathcal{N}_{<0}(\chi_{\rm eff}; \sigma_{\chi_{\rm eff}}) + \zeta_{\rm pos}\mathcal{N}_{>0}(\chi_{\rm eff}; \sigma_{\chi_{\rm eff}})\,.$$

$$f(\chi_{eff}) \sim \mathcal{N}(\bar{\chi_{eff}}, \sigma_{\chi_{eff}})$$

Roulet et. al., (2021)

Also: Galaudage, S., et. al. (2021)

	Δ max ln L	Δ ln Z
Symmetric $\chi_{\rm eff}$	0	0
Positive $\chi_{\rm eff}$	$2.1^{+0.5}_{-0.4}$	$1.6^{+0.5}_{-0.3}$
Positive/Negative mixture $\chi_{\rm eff}$	$2.1^{+0.5}_{-0.4}$	$1.4^{+0.4}_{-0.2}$
Gaussian $\chi_{\rm eff}$	$0.2^{+0.7}_{-0.6}$	$-0.2^{+0.6}_{-0.8}$

Interesting future directions

- The improvements to the LIGO detector have largely left the low-frequency noise (<~60-70Hz) unaffected between the O2-O3 runs. What could be the reason?

- If this is mitigated and we approach “design” sensitivity, we should generically see more cycles in BBH waveforms. Are current waveform models good enough to analyze these signals?

- Can we include more physics (orbital precession + higher harmonics) into the signal models for searches?

Summary

- The availability of the LVK data gives everyone in the community the opportunity to try out and propose new ideas and methods.

- We developed a new end-to-end analysis pipeline that incorporates several innovations

- We achieved an improvement in sensitive volume as quantified by the false alarm rates of known events and injections

- We have new candidate events in all the observing runs, above the thresholds for detection as defined by the LVC

- We also find interesting new results when we analyze the astrophysical population - the distribution of effective spins suggests a preference for positively aligned vs negatively aligned spins in the population